International Journal of Naval Architecture and Ocean Engineering 14 (2022) 100441

Contents lists available at ScienceDirect

International Journal of Naval Architecture and Ocean Engineering

journal homepage: http://www.journals.elsevier.com/international-journal-of-naval-architecture-and-ocean-engineering/

Sensitivity analysis of design parameters for reliability assessment of offshore wind turbine jacket support structures

Abdulhakim Adeoye Shittu [a, b, *], Ali Mehmanparast [c], Peyman Amirafshari [c], Phil Hart [a], Athanasios Kolios [c]

[a] Energy and Power Theme, School of Water, Energy and Environment, Cranfield University, Cranfield, Bedfordshire, United Kingdom
[b] Department of Mathematics and Statistics, Federal University Wukari, Wukari, Taraba, Nigeria
[c] Department of Naval Architecture, Ocean and Marine Engineering, University of Strathclyde, Glasgow, United Kingdom

ARTICLE INFO

Article history:
Received 12 April 2021
Received in revised form
10 January 2022
Accepted 14 February 2022
Available online 17 February 2022

Keywords:
Stochastic sensitivity assessment
Stochastic FEA modelling
Non-intrusive formulations
Iterative FORM
Offshore wind structures

ABSTRACT

Offshore Wind Turbine (OWT) support structures are subjected to hostile environments, defined by highly stochastic loads and complex soil-structure interaction, and thus the need for a probabilistic approach towards design. The study carried out herein presents the sensitivity analysis of these inherent stochastic variables imposed on a complex OWT support structure via purpose-developed modular non-intrusive structural reliability assessment formulation. The results from this study reveal that the uncertainties in the wind speed is a structural design driving factor and the hydrodynamic load effects are secondary to this, for the ultimate (ULS) and Fatigue Limit States (FLS) while their relative sensitivities on the Serviceability Limit State (SLS) cannot be clearly distinguished but are seen to have a dominant impact. Also, it was inferred that incorporating correlation between the variables have a significant impact on the reliability of the structure in the ULS design.

1. Introduction

Research on the design of jacket structures are based on studies that took place 3-4 decades ago, and the new application to offshore wind, with serial production of units and increased operational loads, have re-established the issue of advanced methods of design to be very relevant in current research and practice. Furthermore, stronger and more steady winds found offshore and the reduced need for land area are substantial advantages compared to onshore wind installations. In recent years, studies have mainly focussed on the use of monopiles for offshore wind turbine applications, thereby making detailed studies on the use of jacket foundations an aspect open to further investigation (Shittu et al., 2020a, 2020b; Zwick, 2015; Kolios et al., 2016; Damiani and Song, 2013; Coccon et al., 2017).

A majority of the deployed Offshore Wind Turbines (OWTs) use monopile support structures due to their simple but robust design, especially at water depths less than 50 m. However, monopiles become progressively uneconomical, basically due to modal requirements, which forces the structural dimensions to grow beyond fabrication and installation capabilities currently available as the turbines become larger (>5 MW) and as water depth increases beyond 35–50 m (Kolios et al., 2016; Damiani and Song, 2013; Martin et al., 2013). This has spirited the search for alternative foundations, which can resist extreme environmental factors often imposed on such structures and overcome the drawbacks mentioned above. Structural space frames such as jackets, used extensively in the oil and gas industry, offer a light yet a stiff alternative to monopiles. However, given turbine system dynamics, coupled with the inherent highly stochastic loads, the effective design of these structures is resource-intensive. Therefore, although jacket foundations could go a long way in solving challenges in the offshore wind industry, research is still necessary to support their basic design and analysis (Damiani and Song, 2013; Damiani et al., 2013) also considering factors such as the requirement for optimisation due to the serial production required and the nature of these unmanned structures (Shittu et al., 2020a).

Since modern structures require more complex and reliable designs, it becomes increasingly imperative to propose an accurate and efficient approach to assess uncertainties in material properties and operating environments. In recent years, reliability analysis as a

* Corresponding author. Energy and Power Theme, School of Water, Energy and Environment, Cranfield University, Cranfield, Bedfordshire, United Kingdom.
E-mail address: adeoyeshittu@fuwukari.edu.ng (A.A. Shittu).
Peer review under responsibility of The Society of Naval Architects of Korea.

https://doi.org/10.1016/j.ijnaoe.2022.100441

form of uncertainty analysis has been a valuable tool in structural design because it can directly quantify the effect of uncertainty about input parameters on structural performance (Huang et al., 2018; Kang et al., 2016; Zhang et al., 2015; Zhao et al., 2017; Kolios et al., 2018; Leimeister and Kolios, 2018). Because of this, reliability-based design optimisation has seen increasing interest (Far and Huang, 2019). In the reliability-based design optimisation process, the probability of failure is limited to a target level to minimise the failure risk (Shittu, 2020).

For reliability analysis, given an arbitrary limit-state function $Z = g_X(\boldsymbol{X})$, the Probability of Failure (POF), P_f, can be described as a multi-dimensional integral, which is given by

$$P_f \equiv Pr(g_X(\boldsymbol{X}) \leq 0) = \int \ldots \int_{g_X(\boldsymbol{x}) \leq 0} f_X(\boldsymbol{x}) d\boldsymbol{x} \tag{1}$$

where $Pr(.)$ is a probability function, $\boldsymbol{X} = [X_1, \ldots, X_n]^T$ is an n-dimensional random vector where the upper case X_i denotes it is a random variable and the lower case x_i denotes it is the realisation of the random variable X_i, $f_X(\boldsymbol{x})$ is the joint Probability Density Function (PDF) of the random variables $\boldsymbol{X}$.

Generally, since the convolution integral shown in Eq. (1) is complicated, and of high dimensionality, analytical and direct numerical methods cannot solve it directly. Due to the difficulty in computing this probability function, various methods have been developed over the past few decades. Out of all these methods, the First-Order Reliability Method (FORM) is most prevalent. FORM approximates the true limit state function at the Most Probable Point (MPP), the point on the limit state surface nearest to the origin in the standard normal space. This process enables FORM to work with a good balance between efficiency and accuracy. Because of this good balance, it has become a basic method for reliability analysis (Huang et al., 2018; Breitung, 1984; Lu et al., 2010; Periçaro et al., 2015).

One of the main steps in solving an optimisation problem is determining search direction based on function gradients, referred to as sensitivity analysis. Derivative-based approaches, where parameter sensitivity is measured in terms of the change in model output with respect to an incremental change in the input, are most common in the literature due to their efficiency (Velarde et al., 2019). According to (Velarde et al., 2019; Kala, 2011; Teixeira et al., 2019), other approaches include linear regression of Sobol's decomposition method, Monte Carlo simulations, Morris screening, and variance-based methods. Sensitivity analysis demonstrates changes in the quantity of reliability in terms of variations in stochastic variables. Sensitivity analysis is also used to identify the most significant uncertain variables that have the highest contribution to reliability. Furthermore, sensitivity analysis could be used to provide information for reliability-based design (Xiao et al., 2011).

In general, sensitivity analysis studies the relationship between information flowing in and out of the model. Sensitivity analysis in reliability refers to how uncertainty in the model output can be decomposed into different sources of uncertainties in the model inputs and model uncertainty. The basic categorisation of sensitivity analysis is the deterministic sensitivity analysis and the stochastic sensitivity analysis (Kala, 2011). Ideally, limit state analyses are performed using integrated structural models to capture the complex interactions between the Offshore Wind Turbine (OWT) structure and the environment. Despite uncertainties related to parameter estimation and mathematical representation of wind, wave, soil and structure, deterministic approaches are typically performed by utilising partial safety factors which account for load and resistance uncertainties. On the other hand, probabilistic design approaches allow more rigorous consideration of parameter uncertainties, particularly site-specific environmental inputs, at the expense of higher calculation times. In this regard, identifying the most important sources of uncertainties, i.e., performing a stochastic sensitivity analysis of a complex non-linear model, becomes important (Velarde et al., 2019).

Structural models to determine the response of support structures for OWT can be roughly classified into two groups, namely one-dimensional (1D) beam models and three-dimensional (3D) Finite Element Analysis (FEA) models. In the 1D beam model, the structure is discretised into a series of elastic Euler or Timoshenko beam elements. It is computationally efficient and can be used to accurately model the global structural behaviour, such as evaluating deflections and modal frequencies (Wang et al., 2014). It, however, calculates local structural responses such as stress concentration effects with compromised precision (Petrini et al., 2010). In the 3D FEA model, the support structure is usually described by the application of brick or shell elements. In comparison to the 1D beam model, the 3D Finite Element Analysis Model (FEM) can assume detailed stress distributions and capture structural responses within the structure accurately. The 3D FEM has been applied extensively to wind turbine foundations' structural modelling due to its high fidelity (Shittu et al., 2020a; Wang et al., 2015, 2016a, 2016b, 2017; Gentils et al., 2017; Achmus and Abdel-Rahman, 2005; Kolios and Wang, 2018). Thus, in this study, the 3D FEA model is employed to evaluate the structural responses of the OWT jacket support structure.

Because OWT jacket foundations are embedded through piles into the soil system, it becomes essential to account for soil-structure interaction to capture their structural response adequately. A straightforward method of modelling the soil is by assuming equivalent springs having stiffness based on soil properties, and this approach is known as the p-y method. However, this method tends to underestimate the deflection and the modal frequency (Hyldal, 2012; Hald et al., 2009). A reliable way of modelling the soil system is by assuming 3D FEA with brick elements to obtain accurate and reliable results (Shittu et al., 2020a; Jung et al., 2015; DNV, 2016a). Due to its high efficacy, the 3D FEA with brick elements is adopted in this study to model the soil.

This work aims to conduct a Stochastic Sensitivity Assessment (SSA) for a typical OWT jacket type support structure considering various limit states and stochastic variables. A generic reliability assessment framework, which combines parametric FEA modelling, response surface modelling and reliability analysis specifically for complex OWT jacket type support structures in the presence of highly stochastic variables, has been developed by the authors and will stand as the basis for this study. The adopted method proposes a non-intrusive stochastic formulation, linking the structural model to a reliability analysis algorithm through approximation modelling. A quadratic response surface modelling is adopted to map the structure's response in the domain of stochastic variables. The benefit of this approach is that it allows for high fidelity computational tools to be employed for the analysis, hence extending its applicability to various specialist engineering problems through the advanced modelling techniques and further permitting coupling with analytical reliability methods such as FORM/SORM to allow for low values of probability of failure to be calculated, thus allowing sensitivity assessment based on derivatives (Shittu et al., 2020a). The variables considered in the sensitivity analysis include the wind speed (V), tilting (M_{Tilt}) and torsional moments (M_{Tors}) due to aerodynamics, significant wave height (H_s), Young's modulus (E_{Si}) of each soil strata, Rotor-Nacelle Assembly (RNA)/self-weight (W_i), and the peak wave period (T) (DNV, 2016a; V) Det Norske Veritas. (2005); –J101 Design o, 2014; V) Det Norske Veritas. (1992); Det Norske Veritas. Envir (2000); DNV, 2016b).

In Ref. (Far and Huang, 2019), an algorithm to evaluate the derivatives of safety index and failure probability with respect to the mean, standard deviation, and constant input parameters based on the Advanced First-Order Second-Moment (AFOSM) reliability method was presented. Their work aimed at addressing the drawbacks of existing methods, such as being computationally costly due to their inability to explicitly compute derivatives because the probability of failure is a non-classical parameter function. Therein, to elucidate the modelling process of the proposed program, two examples were presented and solved via spreadsheet application. The same authors, however, stated that their proposed method suffers from the same drawbacks inherent in the AFOSM method, such as its inaccuracy in solving problems involving implicit as well as highly non-linear performance functions.

In Ref. (Ivanhoe et al., 2020), an SRA framework was developed to evaluate the structural integrity of the NREL 5 MW OC4 jacket support structure in the presence of stochastic loads for several limit states. In the same study, for the fatigue LSF, the S−N curve parameters were the intercept (A) assumed to be 12.75, slope (m) equal to 3, and cycle number $N \leq 107$. Their study does not consider critical parameters such as wind speed, wave height, peak wave period but rather the rotor thrust, and hydrodynamic load, among others, in the sensitivity analysis exercise performed therein. Further, the sensitivity analysis considered only the mean and standard deviation values of the stochastic parameters of interest varied to examine the RI sensitivity compared to the defined threshold. The stochastic variables in their study assumed only normal distributions.

In (Shittu et al., 2020a), two SRA frameworks were studied, examined and compared wherein a baseline 10-MW jacket foundation was selected as a reference application. The six-sigma analysis function with Latin hypercube sampling direct simulation approach was employed to predict the failure probabilities in the first approach. In the second, a developed non-intrusive stochastic method wherein the RSM was employed in mapping the structural response model was applied to derive the safety margin, and then applies the First-Order Reliability Method (FORM) to calculate the safety index and, subsequently, the failure probability of the structure. The fatigue LSF in the study assumed the thickness-corrected cathodic-protected D curve given by DNV−OS−J101. The intercept (A) and slope (m) of the S−N curve used for studying the fatigue life of steel structure in seawater for $N > 106$ are given as 15.606 and 5, respectively. The same authors assert that the proposed non-intrusive SRA formulation enhances faster calculations, evaluation of time-variant fatigue reliability index, and the prediction of low failure probabilities for complex engineered structures such as OWT jacket foundations studied in the present paper. The present article is a continued effort from the authors' recent research performed in Ref. (Shittu et al., 2020a).

To the best of the authors' knowledge, the work presented herein is the first of its kind which examines the behaviour of the OWT structure in the presence of parameter uncertainties measured in terms of CoVs as well as the influence of correlation between the crucial parameters on the reliability performance of the structure. The novelty of the current study is evidenced by incorporating the FORM-based SSA with a novel non-intrusive formulation bespoke for 10-MW OWT jacket support structures to enhance the accuracy of the calculated SSA results. This methodology is state-of-the-arts because facilities inbuilt in the ANSYS software package such as the high-fidelity Design Explorer©, which facilitates stochastic parametric FEA by employing new DoE techniques are coupled with the iterative FORM through MPR entirely coded as MATLAB routines to calculate the sensitivity indices of the structure. This can be applied to non-linear problems and those characterised by implicit LSF aside from an added advantage of allowing unusual random input parameters such as wind speed, wave height, and peak wave period, to name a few to be entered into the analysis. Apart from accounting for the sensitivities of the structural design parameters, the framework developed in this study also accounts for their uncertainties measured in terms of CoVs in contrast to previous sensitivity analysis works in Refs (Far and Huang, 2019; Ivanhoe et al., 2020). wherein their sensitivity analysis neither provides explicit information about the rate of change in the reliability or failure probability due to changes in the variables, such as means and standard deviations, of distributions nor examine these phenomena as they vary with a wide-set of uncertainties measured in terms of CoVs as investigated in the present paper. This study further examines the interactive effects of the random input variables on the reliability performance of a complex frame type structure for OWTs, considering several limit states. Besides assuming normal distributions, the developed stochastic framework in the current study also applied non-normal stochastic variables. Further, the present study overcomes the limitations inherent in the AFOSM method, such as its inaccuracy in solving problems involving implicit as well as highly non-linear performance functions as this study develops an integrated RSM-iterative FORM SSA algorithm to provide a best-fit limit state surface (LSS) corresponding to the data of interest bespoke for OWT support structures. This enhances the accuracy of the calculated sensitivity estimates.

The rest of the present paper is organised as follows: Section 2 introduces the design load analysis where the sources of loads and design load cases are discussed; Section 3 discusses the parametric FEA built for the OWT, highlighting the geometry, mesh, material, and boundary conditions used, as well as the validation of the FEA model; Section 4 highlights the implementation of the steps of the proposed stochastic sensitivity analysis discussing the non-intrusive formulation and the SSA based on the iterative FORM; In section 5, results obtained from the study are discussed extensively; and finally, Section 6 draws the main conclusions of the work conducted.

2. Design load analysis

2.1. Sources of loads

OWTs are subjected to several load sources imposed by their environment and operational activity. A list of loads to be accounted for in the design of OWT jacket support structures are set out in design standards, such as DNV−OS−J101 (–J101 Design o, 2014) and IEC 61,400−3 (Wind, 2009). Calculations and formulations of each load produced by the environment will, in this study, be based on DNV-RP-C205 (Det Norske Veritas. Envir, 2000). The relevant loads imposed on OWT support structures can roughly be classified into six groups, i.e. (1) aerodynamic loads transferred from the rotor; (2) wind loads on the tower; (3) inertia loads; (4) current load; (5) wave loads and (6) hydrostatic loads (Gentils et al., 2017). These loads are illustrated in Fig. 1.

Gravitational and inertia loads are static and dynamic loads resulting from gravitational pull, such as the mass of the whole structure and equipment imposed on the structure under operation and the forces acting on the structure as a result of operations (Minguez, 2015). The inertia loads, resulting from the weight of the support structure and RNA at the tower top, can significantly impact the buckling and influence the eigen-frequencies of the OWT foundation (Gentils et al., 2017).

Aerodynamic loads are dynamic and static loads occurring as a result of the interaction between the airflow and the moving and stationary components of the wind turbine. The magnitude of the

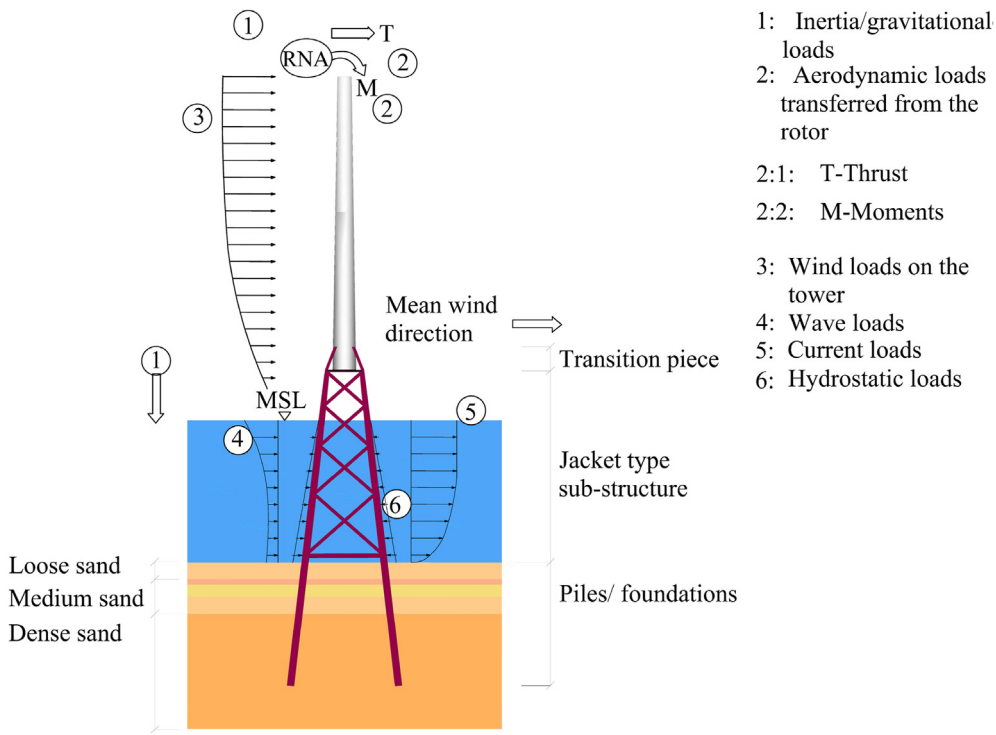

Fig. 1. Schematic of the loads on the OWT jacket support structure embedded in layered soil showing the geometry.

load varies and depending on the air density, the mean wind speed and turbulence across the rotor plane, and the aerodynamic shapes of the components of the wind turbine and their interactive effects. These loads are determined by using aero-elastic load models (Wang et al., 2014; Minguez, 2015; Jalbi and Bhattacharya, 2020). The aerodynamic loads produced by the rotor pushes the tower at the top and are often decomposed into a load matrix defined in the referential axis of the wind turbine. The fatigue loads were evaluated by adopting the Damage Equivalent Load (DEL) method, explained in (Freebury and Musial, 2000). A thrust load in the same direction as the diagonal of the base of the jacket was imposed on the support structure and applied at the assumed RNA Centre of Mass (CM). The aerodynamic loads, such as the M_{tilt} and M_{tors} can be calculated from parameters such as the yaw error and tilt angle. Since the RNA coupled with the blades for the turbine is usually large, and considerable eccentricity is created due to the lateral span of this assembly impose these moments. Parameters such as the turbulence intensity, tilt angle, wind gust, and wind direction have been accounted for in the analysis whilst carrying out the stochastic model calculations in terms of the input parameters: M_{tilt} and M_{tors}.

This loading set-up is assumed to resemble a yaw error situation to produce an additional moment due to torsion at the top of the tower. This was carried out in the presence of a horizontal offset for the RNA CM, which led to a moment due to gravity at the top of the tower (Damiani et al., 2013). Wave load and rotor thrust vectors were applied in the same direction as the jacket base diagonal so that the maximum compression and tension effects are produced on the opposite legs (Shittu et al., 2020a; Damiani and Song, 2013).

Environmental loads are those caused by environmental phenomena, i.e., the set produced by wave force, current force and wind force. Wave loads are dynamic loads resulting from waves and their interaction with the OWT support structure. Typically, bottom-fixed offshore structures are dominated by drag owing to the wavelength, water depth, structural shape and size; thus, Morison's Equation is employed. Morison's Equation assumes that the total wave force exerted on a structure can be calculated by the linear superimposition of the drag and inertia forces. To evaluate the wave loads which acts on the structure using Morrison's Equation, the member diameter, D, has to be less than one-fifth of the wavelength, λ, i.e.:

$$D \leq 0.2\lambda \tag{2}$$

Current and wave loads can be calculated using Morison's Equation thus, for slender members such as components of jackets submerged in water (–J101 Design o, 2014):

$$F = F_d + F_m = \frac{1}{2}\rho_w C_d D|u_x|u_x + \rho_w C_m \frac{\pi D^2}{4} a_x \tag{3}$$

where the drag force is the first term while the inertia force is the second term; ρ_w is the density of water; C_d and C_m are the piles' coefficients of drag and inertia, respectively, and their corresponding values are 1.25 and 2.0 respectively (Damiani and Song, 2013); D is the cylinder diameter; a_x and u_x are the horizontal wave-induced or current-induced acceleration and velocity of water, respectively which were derived from the regular wave theory.

Current loads can be described as dynamic loads emanating from the water flow from external sources other than surface waves. Current can lead to drag loads being induced on the support structure. The current velocity $u_c(z)$ is assumed to follow a subsurface current exponential profile from the seabed, d to the Mean Sea Level (MSL). The total current velocity of a submerged, stationary, tubular member, in the absence of vortex shedding, can be computed thus:

$$u_c(z) = u_{c,MSL}\left(\frac{d+z}{d}\right)^{1/7} \tag{4}$$

where, $u_{c,MSL}$ is the current velocity at MSL, d is the depth of water from MSL to the seabed. The wave-particle velocity and the current velocity are summed up in Morison's equations drag term in Eq. (3), assuming that the wave and current act in the same direction. The wind loads pushing the tower structure results from the drag and are a function of the average wind velocity $\overline{V}(z)$. Generally, the wind shear is described by a power-law profile and can be determined from the following Equation:

$$\overline{V}(z) = \overline{V}_r\left(\frac{Z}{Z_r}\right)^{\alpha} \tag{5}$$

where $\overline{V}_r$ represents the reference wind speed at the elevation of nacelle altitude Z_r, and α, which has a value of 0.115, is the roughness coefficient for the offshore site (Gentils et al., 2017). Wind loads exerted along the tower can be computed, thus:

$$F_{tower}(z) = \frac{1}{2}\rho_a C_{D,T} D(z)\overline{V}_r^2(z) \tag{6}$$

where $C_{D,T}$ which is taken as 1.0 is the coefficient of drag of the tower, $D(z)$ denotes the external diameter of the tapered tower at height z. Having calculated the wind load, the moment due to the effects of the wind load can then be determined.

Hydrostatic pressure exerted on the submerged members of the jacket foundation is a constant normal load and varies with the depth of water. The hydrostatic force can be calculated from:

$$F_h = \rho_w g h \tag{7}$$

where F_h is the hydrostatic force, g is the acceleration due to gravity, and h is the water depth.

2.2. Design load cases (DLCs)

The DLCs should cover a set of design situations taking into consideration the most severe conditions that an OWT foundation is likely to be subjected to, combining extreme or standard external conditions with operational states of the wind turbine or other operational modes (such as installation, transportation, fault, or maintenance) (Minguez, 2015). Thirty-two (32) DLCs are set out consisting of all modes of operation of an OWT in IEC61400-3 (Wind, 2009) for the structural design of OWTs, including start-up, standard operation, shut down and 50-year extreme conditions. These DLCs can be classified roughly into two main groups, namely, ultimate and fatigue. Typical load cases employed, basically, in the structural design for OWTs foundations are mainly by assuming the fatigue loads based on normal sea states while assuming the ultimate load based on a 50-year extreme condition. According to (DNV, 2016a), the serviceability load cases can be determined as specified in (DNV, 2016b). For simplicity, both the ultimate and fatigue load cases are considered in this study.

2.2.1. Ultimate load case

The load derived from the 50-year return period is commonly assumed to be a critical ultimate load case for the extreme hydrodynamic loads experienced by OWT. A previous study (Freebury and Musial, 2000) revealed that wind loading is a design driving factor for a typical OWT rather than hydrodynamic loading. Hence, it is usually assumed that the critical load case for ULS is defined by the parked turbine, under the 50-year EWM (extreme wind model) with 50-years RWH (reduced wave height) and ECM (extreme current model). The loading characteristics, as described above, corresponds to the IEC 61400−3 (Wind, 2009) DLC 6.1 b and 2.1 GL regulation (Rule, 1995), respectively. Load safety factors for gravitational and other loads (such as environmental loads) are 1.1 and 1.35, respectively (61400-1: Wind Tu, 2005; Fisher et al., 2010).

2.2.2. Fatigue load case

During the life of OWTs, a significant source of periodic loadings acts on the structure due to the nature of rotor operation as well as hydrodynamic loading. Hence, there is a high risk of OWT foundations failing by fatigue (Gentils et al., 2017; Muskulus and Schafhirt, 2310). A widely used fatigue DLC correlates to an operating state within the Normal Sea State (NSS) and Normal Turbulence Model (NTM). The site is assumed to have no current, and the significant wave height and the cross zero periods are obtained via a probability density function of the site. DLC 1.2, as specified in the IEC standard (Wind, 2009), are generally regarded as the governing fatigue DLCs for OWT support structures. Therefore, they are considered in this study as fatigue load cases (Gentils et al., 2017; Lee et al., 2014). According to the IEC standard (61400-1: Wind Tu, 2005; Fisher et al., 2010), the safety factor for fatigue load is equivalent to 1.0.

3. OWT case study

Given the exorbitant cost of support structures and related Operation and Maintenance (O&M) activities, there is continued interest in increasing the size of offshore turbines. The OWT (Damiani and Song, 2013; Damiani et al., 2013; JacketSE, 2016) is assumed to be a simple reference 10 MW turbine scaled from a 5 MW (National Renewable Energy Laboratory) NREL reference turbine (Jonkman et al., 2009). The main properties were calculated through basic mechanics considerations and scaling laws. An 88.4 m tapered tubular tower supports the RNA. Its essential characteristics and other data as applied in this study are derived from (Damiani and Song, 2013; Damiani et al., 2013).

3.1. Parametric FEA

The Finite Element Analysis Method is a very powerful option for designing modern engineering structures capable of developing a reliable model for predicting such systems' behaviour in a cost-effective time scale. The ANSYS software package is a well-established multi-purpose FEA software used to build a parametric Finite Element Analysis Model (FEM) of the OWT foundation and the soil system. The parametric FEM enhances the modelling of OWT structures with stochastic variables, such as material properties and environmental parameters. The parametric FEM represents the jacket support structure of the 10-MW OWT, where the main parameters and other details are derived from (Shittu et al., 2020a, 2020b). The wind and wave loads, which are environmental loads, are calculated and then applied to the structure in an uncoupled way, such that fluid-structure interactions are ignored. The geometry, mesh and boundary conditions used in the FEM are presented in the next subsections (Shittu et al., 2020a).

3.1.1. Geometry

The jacket configuration is usually a space frame with four legs, inter-connected with bracings welded together. The structural assembly comprises a transition piece that transfers the forces from the tower into the submerged jacket structure, anchored via piles or suction caissons, to the seabed at each leg. The TP is assumed to be a deck reinforced by stringers that supports a central cylindrical shell supported by four tubular struts. The principal geometric

dimensions of the structure studied herein are presented in Table 1.

3.1.2. Mesh

The mesh generation is an essential step in coupling the model to be used for the FEA. The ANSYS software package provides a powerful and reliable structure mesh generator capable of developing a consistent mesh structure with minimal computational requirement. In order to ensure the accuracy of results, the mesh is optimised by performing a mesh sensitivity analysis. From the mesh sensitivity study, the Equivalent (von-Mises) Stress converged at the mesh size of 2 m for the soil and 0.5 m for the support structure, corresponding to a total number of elements of 190,222. Hence, 2 m and 0.5 m are deemed as suitable mesh sizes for the soil and the support structure, respectively. Further details about this analysis as applied in this study can be found in (Shittu et al., 2020a). As applied in the present parametric FEA, other crucial information such as the material properties, site specifications, and soil profile is derived from (Shittu et al., 2020a, 2020b).

3.1.3. Boundary conditions

A load matrix with the aerodynamic loads is applied at the tower top, and the wind and wave loads are applied to the tower surface and the support structure surface submerged into the water, respectively. Additionally, the following three boundary conditions are also defined: (1) the bottom of the soil model is fixed against translation in all directions; (2) the soil model's lateral boundaries are fixed against lateral translation; (3) an augmented Lagrangian formulation-based frictional contact (nc. Introduction t, 2010; help documen, 2018) is established between the soil and pile with suitable friction coefficients to enable soil-structure interaction.

Since the detailed modelling of the nacelle's and rotor's (composed of the hub and blades) is not part of the parametric model, they are entered into the FEA as distributed or concentrated masses so as to be able to simulate the OWT's structural behaviour accurately. It is not necessary to model the blades since, besides the mass added to the tower top, parked and feathered blades have negligible impact on the natural frequency of the OWTs (Martinez-Luengo et al., 2017).

Table 1
Principal geometric dimensions for the baseline 10-MW support structure (Shittu et al., 2020a). MSL – mean sea level; OD – outer diameter; WL – wall thickness; TP – transition piece.

Parameter	Value
Deck height above MSL (m)	16
Water depth (m)	50
Leg OD (m)	1.74
Leg WT (m)	0.030
Number of bays	4
Jacket batter	8.47
Height of TP (m)	7
Number of legs	4
Pile OD (m)	1.59
Pile WT (m)	0.037
Mud brace OD (m)	0.762
Mud brace WT (m)	0.017
x-brace OD (m)	0.61
x-brace WT (m)	0.016
Tower length (m)	88.4
Tower-top OD (m)	3.85
Tower-top thickness (m)	0.03
Tower-base OD (m)	7
Tower-base thickness (m)	0.055

3.2. Validation of the FEA model

3.2.1. Modal analysis

Taking into consideration the analysis of the natural/modal frequencies (Eigen-frequencies) accounting for self-weight of the entire structure, a comparison is made between the present FEA model and values found in the literature (Damiani and Song, 2013; Damiani et al., 2013; JacketSE, 2016). As can be observed in Table 2, from the first and second fore-aft and side-to-side modal frequencies obtained from the present FEA model, a good agreement with the values found in literature is achieved with the observed maximum percentage difference being 11.11% for the second side-side mode. Therefore, the present FEA model validation is achieved. See Fig. 2(a).

3.2.2. Deflection in static analysis

This subsection of the validation exercise aims to examine, in a static analysis, the deformation behaviour of the support structure. As derived from (Damiani and Song, 2013; Damiani et al., 2013), the RNA weight and a 3.4 MN thrust load were applied on the tower top. The displacements at the RNA elevation and the base of the tower are compared with reference values, and results are reported in Table 3. Under the loaded condition, the deflections at the RNA and base of the tower were measured with respect to the location of the RNA and centre of the base of the tower, respectively.

As can be observed from Table 3, a good agreement is achieved when making a comparison between the present FEA model's results and the reference values reported in (Damiani et al., 2013), for both deflections at the RNA and base of the tower, with an observed maximum difference of 3.44% for deflection at the base of the tower. Therefore, the validity of the present FEA model is further confirmed. See Fig. 2(b).

3.3. Validation of the reliability SSA model

To validate the fact that the fatigue RI is sensitive to CoV, with reference to Fig. 3 below in the current paper, it can be observed that the RI recorded at CoV = 0.095, CoV = 0.1 and CoV = 0.105 corresponds to RI = 4, RI = 3.9 and RI = 3.8, respectively. In comparison, with reference to Fig. 11 in Ref. (Shittu et al., 2020a), it can be observed that the RI recorded at CoV = 0.095, CoV = 0.1, and CoV = 0.105 corresponds to 4, 3.92 and 3.843, respectively. Hence, the result obtained in the study matches very well with that obtained in Ref. (Shittu et al., 2020a).

4. The application of the stochastic sensitivity analysis (SSA) on the OWT support structure

In this section, the structural reliability sensitivities of stochastic variables for the OWT support structure is assessed considering five limit states, according to DNV–OS–J101 (–J101 Design o, 2014). The fully parametric FEA model presented in section 3.1 is employed in developing the FEA model taking into consideration the stochastic variables. The results are then post-processed using a non-intrusive formulation developed for the purpose of SSA in this study (Shittu et al., 2020a).

4.1. Limit state design criteria

As set-out in DNV–OS–J101, it is important to safeguard the structure against failure resulting from the violation of three limit state conditions for OWT support structures, i.e., (1) ULS (ultimate limit state), which involves designing for maximum loading-carrying capacity (i.e. buckling and yielding stress); (2) FLS (fatigue limit state), which entails safeguarding against failure

Table 2
Modal frequencies of the 10 MW OWT support structure (Shittu et al., 2020a).

Modal frequencies (Hz)	Ref. (Damiani et al., 2013; JacketSE, 2016)	Present	%Diff.
1st fore-aft bending	0.21629	0.22297	2.99%
1st side-to-side bending	0.21320	0.21346	0.12%
2nd fore-aft bending	1.6561	1.5292	−8.29%
2nd side-side bending	1.0313	1.1602	11.11%

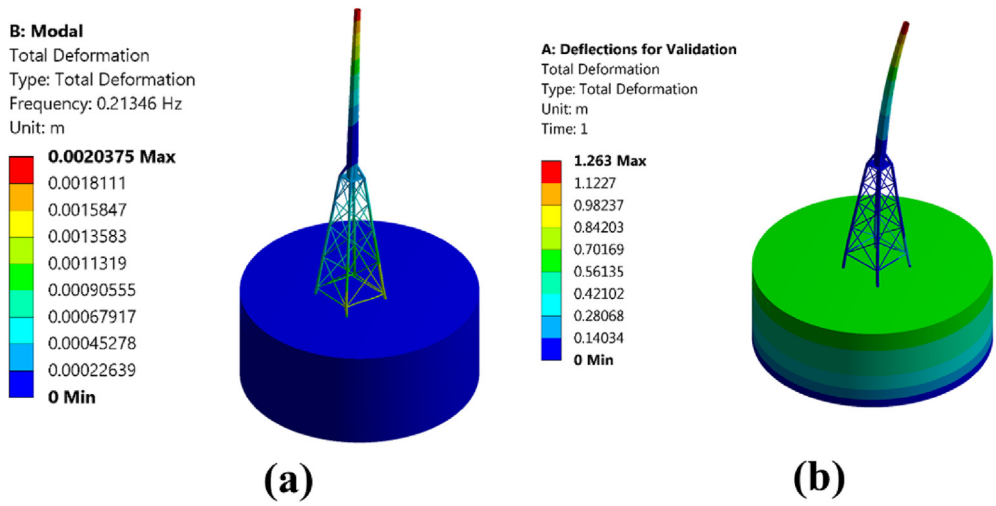

Fig. 2. 3D isometric view of the structural model's (a) first mode frequency and (b) total deformation at RNA elevation (Shittu et al., 2020a).

Table 3
Deformation in static analysis of the baseline 10 MW on jacket (Shittu et al., 2020a).

Load case	Displacement at tower base					
Mass/thrust RNA/3.4 MN	Ref. (Damiani et al., 2013) 1.2688	Present 1.263 m	% Diff. −0.46%	Ref. (Damiani et al., 2013) 1.6639×10^{-1}	Present 1.6085×10^{-1}	% Diff. −3.44%

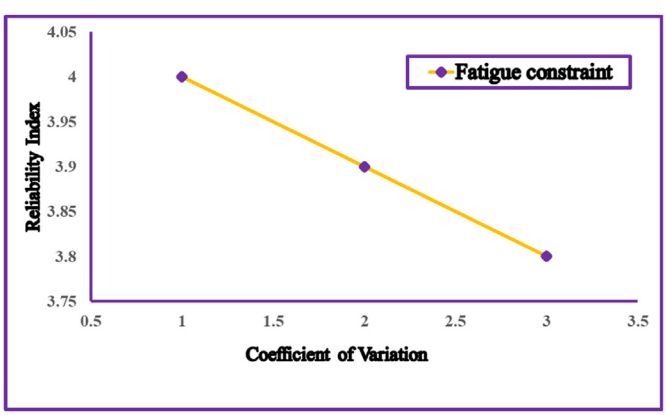

Fig. 3. Variation of the fatigue reliability indices with CoV (design life = 20 years).

resulting from cyclic loads; and (3) SLS (serviceability limit state), which implies attaining tolerance criteria (i.e. vibrations and deflections) acceptable for standard use. Thus, in this study, the structural reliability sensitivity assessment of OWT support structures takes into consideration five design criteria, i.e. stress (ULS), vibration (SLS), buckling (ULS), deformation (SLS) and fatigue (FLS). The location within the structure where the reliability index (RI) results are assessed is detailed in Fig. 4.

4.1.1. Stress limit state

The ULS (ultimate limit state) defines the resistance of the structure against yielding. In terms of the ultimate limit state, the maximum stress in the support structure $\sigma_{VM,\ max}$ should not exceed the allowable stress limits $\sigma_{VM,\ allow}$. The Limit State Function (LSF) for the von-Mises criterion can be expressed as Eq. (8):

$$g_u(x) = \sigma_{VM,allow} - \sigma_{VM,max} \tag{8}$$

The allowable stress $\sigma_{VM,\ allow}$ can be expressed as:

$$\sigma_{VM,\ allow} = \frac{\sigma_y}{\gamma_m} \tag{9}$$

where σ_y is the yield strength, with a value of 355 MPa for steel S355; γ_m is the material safety factor, with a value of 1.1 suggested by DNV−OS−J101 standard (–J101 Design o, 2014). Thus, the allowable stress $\sigma_{VM,\ allow}$ is 323 MPa.

4.1.2. Buckling limit state

The slenderness of the support structure coupled with the large RNA mass and other forces at the tower top necessitates an investigation of the risk of instability as a result of buckling. The ultimate limit state static analysis results are employed as pre-stress loads. The load multiplier L_m which is defined as the critical load divided by the present load applied, should exceed the permissible load multiplier, $L_{m,allow}$ in order to avoid failures. This design criterion is given as:

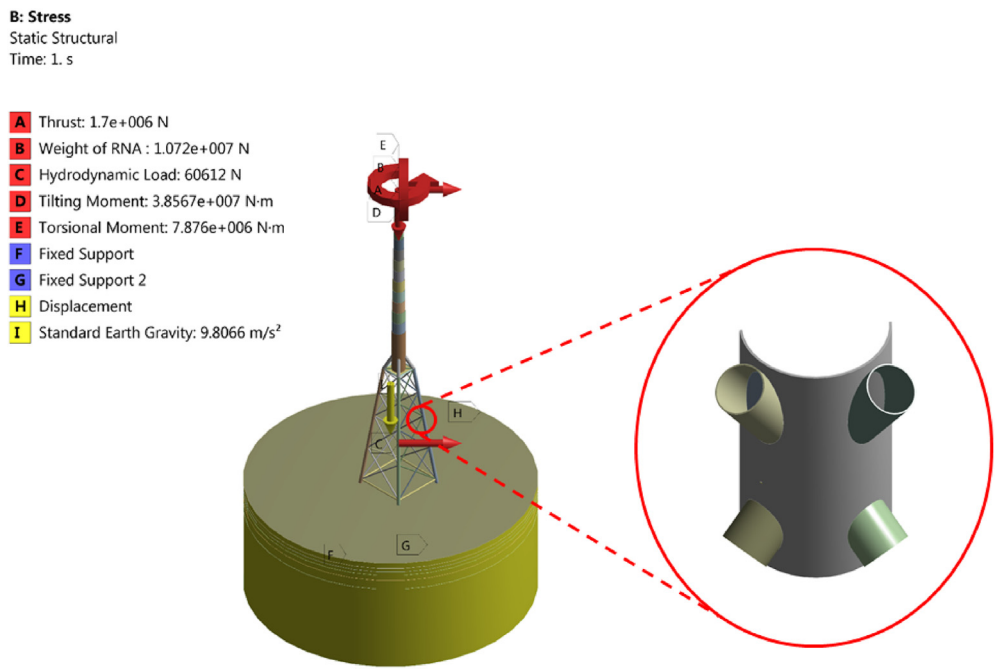

Fig. 4. 3D structural model elucidating the critical location where reliability index results are evaluated (Shittu et al., 2020b; Shittu, 2020).

$$L_m \geq L_{m,allow} \tag{10}$$

According to the DNV standard (DNV, 2016a), 1.4 is adopted as the $L_{m,allow}$ value, in this study. The LSF for buckling criteria can thus be expressed as:

$$g_b(x) = L_m - L_{m,allow} \tag{11}$$

4.1.3. Fatigue limit state

The fatigue limit state is a crucial phenomenon in OWT support structures as they are subjected to significant cyclic loads. OWT support structures normally have a long service period that may exceed 20 years. This, in conjunction with the inspection intervals, affects the reliability requirement of the jacket structural design. According to the S–N curve method, the number of loading cycles to failure, N, can be obtained by:

$$\log N = A - m \log \Delta S \tag{12}$$

where A and m are the intercept and the slope of the S–N curve on the log-log plot, respectively; ΔS is the stress range. The two parameters in Eq. (12), i.e. intercept A and slope m are generally given by design standards, e.g. DNVGL-ST-0126. The LSF of fatigue reliability assessment based on the S–N curve method can be expressed as:

$$g_{f,\,SN} = \log N - \log N_t \tag{13}$$

where subscripts f and SN denote the fatigue limit state and S–N curve method respectively; N is the number of loading cycles to failure given by Eq. (12), N_t is the number of loading cycles expected during the given design life. The number of cycles during the design life N_t may be determined as a function of rated rotor speed n_{rated} and availability η_a (98.5%) on the location chosen (Gentils et al., 2017; Kühn, 1999). Therefore, considering a design life of 20 years, the number of cycles can be expressed as:

$$N_t = \eta_a . n_{rated} \times (20[year] \times 365[day/year] \times 24[hour/day] \times 60[min/hour]) \tag{14}$$

The minimum fatigue safety ratio $f_{sr,min}$ must be greater than the allowable fatigue safety ratio $f_{sr,allow}$ which is equivalent to the product of one and the material PSF (Partial Safety Factor) $\gamma_{m,f}$ for fatigue:

$$f_{sr,min} \geq f_{sr,allow} \tag{15}$$

Since the material's PSF for Fatigue Limit State is 1.15 (DNV, 2016a), $f_{sr,allow}$ is equivalent to 1.15. Hence, the LSF based on the fatigue safety ratio can be expressed as

$$g_{f,f_{sr}} = f_{sr,allow} - f_{sr,min} \tag{16}$$

For the calculation of the fatigue sensitivity index across the nominal service life of the asset, a quasi-static approach is assumed, where the annual reliability sensitivity index can be calculated and plotted accordingly for the 20 years of consideration.

4.1.4. Deformation limit state

Excessive deflections influence the serviceability of OWT support structures and, therefore, should be avoided. The allowable deflection d_{allow} must exceed the maximum deflection d_{max} to ensure overall structural stability. This can be expressed as:

$$d_{allow} > d_{max} \tag{17}$$

The LSF for deflection criteria can be expressed as:

$$g_d(x) = d_{allow} - d_{max} \tag{18}$$

The allowable deflection d_{allow} is given by the following empirical Equation as suggested by DNV–OS–J101 (–J101 Design o, 2014):

$$d_{allow} = \frac{L}{200} \tag{19}$$

where L is the height of the jacket.

4.1.5. Vibration limit state

One of the critical concerns for offshore wind turbines on jacket support structures is the resonance phenomena. In order to design the structure against such phenomena, the first eigen-frequency f_{1st} of the OWT support structure must be separated sufficiently from rotor induced frequencies f_{1P} and blade-passing frequency f_{3P}. A soft-stiff structural design whereby the modal frequency lies between the rotor upper bound f_{1P} (f_{1PH}) and lower bound f_{3P} (f_{3PL}) frequencies is presently the most usual and cost-effective design for jacket. Therefore the resonance constraint could be expressed by (Shittu et al., 2020a; Zwick, 2015; Damiani and Song, 2013; Gentils et al., 2017):

$$f_{1PH} \leq f_{1st} \leq f_{3PL} \tag{20}$$

$$0.133 \leq f_{1st} \leq 0.233 \tag{21}$$

The LSF for the resonance criterion at the rotor lower bound can thus be expressed as,

$$g_r(x) = f_{1st} - f_{1PH} \tag{22}$$

While at the rotor upper bound,

$$g_r(x) = f_{3PL} - f_{1st} \tag{23}$$

The lower g-function value is chosen to be applied in the reliability assessment.

The aero-elastic modelling concept applied in this study was derived from other studies (Wang et al., 2014; Minguez, 2015; Jalbi and Bhattacharya, 2020), which asserted that aerodynamic damping is the result of the relative velocity between the wind turbine structure and the surrounding air. Aerodynamic damping depends on the particular wind turbine and is inherent in aero-elastic load model theories for analysing wind turbine rotors.

4.2. A non-intrusive formulation

The FEA model is used here to perform a series of FEA simulations on the structure with the help of the design of experiments (DoE) module in ANSYS (in the ANSYS DesignXplorer© facility). From the simulations executed on the ANSYS DoE tool, the results are imported into a MATLAB code that has been developed for response surface modelling via the use of multivariate polynomial regression (MPR). In brief, the analysis starts from the definition of the system, associated limit state and determination of which variables will be considered as stochastic in the analysis. Next, a number of FEA simulations is executed by varying inputs and recording outputs related to limit states in order to map the response of the structure in the domain of stochastic variables. An appropriate method is then selected in order to approximate the response of the system and link output variables with global inputs. Finally, the SSA is carried out employing the recursive FORM algorithm. A flow chart of the non-intrusive formulation developed for this study is presented in Fig. 5.

For time-variant limit states, such as fatigue, the steps detailed in the foregoing should be followed in a recursive process calculating the reliabilities annually and hence the reliability for different time periods can be quantified in a quasi-static way (Ivanhoe et al., 2020).

4.2.1. Multivariate regression

Regression analysis is a statistical process for establishing the relationship between a dependent variable and one or more independent variables. Taking the Ultimate Limit State (ULS) stress constraint as an example, the dependent variable (i.e. maximum von-Mises stress, $\sigma_{VM,max}$) and independent variables (i.e. thrust load x_1, tilting moment x_2, torsional moment x_3, total hydrodynamic load (wave) x_4, soil 1 young's modulus x_5, soil 2 young's modulus x_6, soil 3 young's modulus x_7 and weight of RNA x_8) are assumed to have the following functional relationship:

$$\sigma_{VM,max} = [a_0, a_1, \ldots, a_{16}] \begin{bmatrix} 1 \\ x_1 \\ x_1^2 \\ . \\ . \\ . \\ x_8 \\ x_8^2 \end{bmatrix} \tag{24}$$

$(a_0, a_1, \ldots, a_{16})$ in Eq. (24) are $2n+1$ regression coefficients for a quadratic regression. For other types of limit states, i.e. deformation, buckling, vibration and fatigue, expressions similar to Eq. (24) can be derived. Multivariate regression can be used to obtain the regression coefficients for different limit states (Kolios, 2010). The response surfaces for every single component can be produced, but the results for the most critical will be presented here.

In this study, 300 stochastic FEA simulations were performed, obtaining 300 sample sets. The R-square values obtained in the Multivariate Polynomial Regression (MPR) analysis performed in all cases were consistently higher than 0.95, which indicates the success of the MPR. For stochastic simulations, the number of samples is generally chosen between $(2n+1)$ and 3^n, where n is the number of stochastic variables. The larger number of samples generally enables more accurate results but at the expense of high computational costs. In order to achieve accurate results, 300 simulations have been carried out in ANSYS herein, which is larger than $(2n+1)$, obtaining response values of 300 design samples related to the different stochastic parameters chosen (Kolios et al., 2018).

4.3. SSA

Consider the performance function of a component is $G(b, x)$, where b is the design variables and x is the vector of random variables. When FORM is employed for reliability assessment, the probability of failure is calculated as follows (Haldar and Mahadevan, 1999):

$$P_f = 1 - \Phi(\beta) \tag{25}$$

where β is the RI and $\Phi(\cdot)$ is the cumulative density function of the standard normal distribution. Thus, the sensitivity of failure probability with respect to design variable $\left(\frac{\partial P_f}{\partial b}\right)$ can be expressed as:

$$\frac{\partial P_f}{\partial b} = -\varphi(\beta)\frac{\partial \beta}{\partial b} \tag{26}$$

where $\frac{\partial \beta}{\partial b}$ is the derivative of the safety index with respect to design variable (b) and $\varphi(.)$ is the density function of standard normal distribution. One of the most crucial issues in the approximation of

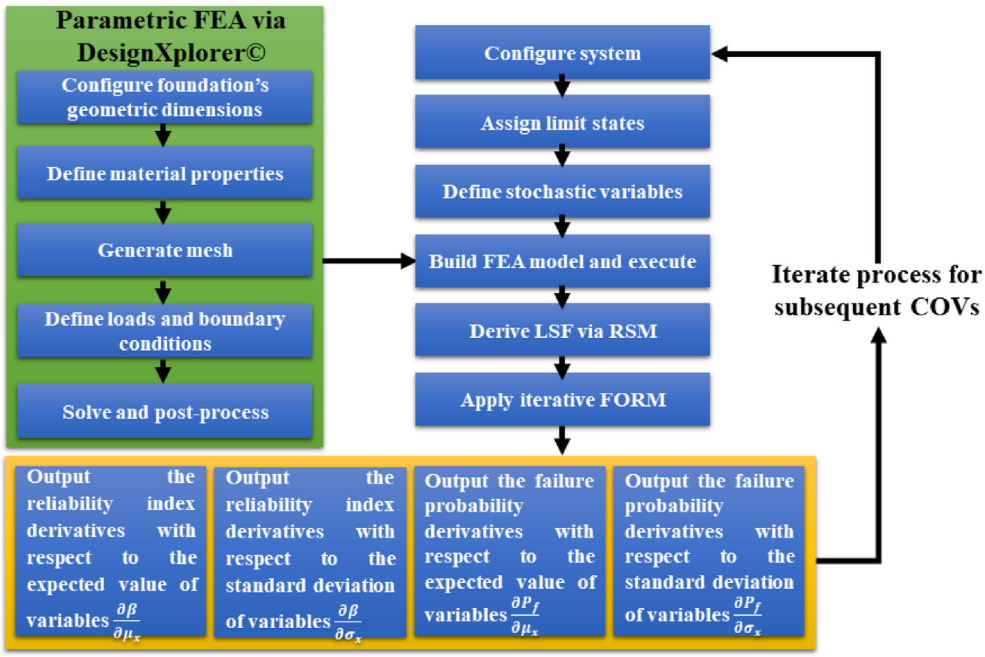

Fig. 5. Flow chart of the modular non-intrusive SSA framework.

sensitivity derivatives is the type of distribution function governing the variables (Melchers, 1999). To address this issue, the input variables are transformed to the normal standard space using the change of variable using Rosenblatt transformation (Melchers, 1999; Ditlevsen and Madsen, 1996). Then, the variables are entered into the algorithm as a vector of equivalent normal variables. This technique allows the algorithm to accommodate a wide range of probabilistic distribution functions. For this purpose, irrespective of the type of distribution function governing the random variables involved, the standard normal form of variables (U), which is widely applied in reliability analysis, is expressed as (Nowak and Collins, 2012):

$$U = \frac{x - \mu_x}{\sigma_x} = \{U_1, U_2, \ldots, U_n\}^T \tag{27}$$

where μ_x and σ_x are the mean and standard deviation of random variables, respectively. Hence, the performance function can be rewritten based on standard normal variables in the form of $G(b,U)$. According to (Kwak and Lee, 1987) the derivative of β with respect to design variable (b), as a general case, can be expressed as:

$$\frac{\partial\beta}{\partial b} = \lambda \frac{\partial G}{\partial U}\frac{\partial U}{\partial b} \tag{28}$$

where λ, the Lagrange multiplier, can be calculated as:

$$\lambda = -\frac{1}{\left|\frac{\partial G}{\partial U}\right|} \tag{29}$$

Meanwhile, two scenarios are considered here:

- The design variable is the mean of the random variables
- The design variable is the standard deviation of random variables

These two cases are examined separately in the next subsections.

4.3.1. Reliability sensitivity with respect to mean

Taking the mean of the random variables as the design variable, b, Eq. (28) can be expressed as:

$$\frac{\partial\beta}{\partial\mu_x} = -\frac{1}{\left|\frac{\partial G}{\partial U}\right|}\frac{\partial G}{\partial U}\frac{\partial U}{\partial\mu_x} \tag{30}$$

The derivative $\frac{\partial U}{\partial\mu_x}$ can be calculated from Eq. (27):

$$\frac{\partial U}{\partial\mu_x} = \frac{\partial}{\partial\mu_x}\left(\frac{x-\mu_x}{\sigma_x}\right) = -\frac{1}{\sigma_x} \tag{31}$$

Employing the chain rule, the derivative $\frac{\partial G}{\partial U}$ can be expanded as:

$$\frac{\partial G}{\partial U} = \frac{\partial G}{\partial x}\frac{\partial x}{\partial U} = \frac{\partial G}{\partial x}\sigma_x \tag{32}$$

Substituting Eqs. (31) and (32) into Eq. (30), $\frac{\partial\beta}{\partial\mu_x}$ can be simplified as:

$$\frac{\partial\beta}{\partial\mu_x} = -\frac{\frac{\partial G}{\partial x}\sigma_x}{\left|\frac{\partial G}{\partial x}\sigma_x\right|}\left(-\frac{1}{\sigma_x}\right) = \frac{\frac{\partial G}{\partial x}}{\left|\frac{\partial G}{\partial x}\sigma_x\right|} \tag{33}$$

4.3.2. Reliability sensitivity with respect to standard deviation

In this section, taking the standard deviation of random variables as design variable, b, Eq. (28) is rewritten as:

$$\frac{\partial\beta}{\partial\sigma_x} = -\frac{1}{\left|\frac{\partial G}{\partial U}\right|}\frac{\partial G}{\partial U}\frac{\partial U}{\partial\sigma_x} \tag{34}$$

Using Eq. (27), the derivative $\frac{\partial U}{\partial\sigma_x}$ is calculated as:

$$\frac{\partial U}{\partial\sigma_x} = -\frac{\partial}{\partial\sigma_x}\left(\frac{x-\mu_x}{\sigma_x}\right) = -\frac{x-\mu_x}{\sigma_x^2} \tag{35}$$

Substituting Eqs. (32) and (35) into Eq. (34), $\frac{\partial\beta}{\partial\sigma_x}$ is obtained as:

$$\frac{\partial\beta}{\partial\sigma_x} = -\frac{\frac{\partial G}{\partial x}\sigma_x}{\left|\frac{\partial G}{\partial x}\sigma_x\right|} \times \left(-\frac{x-\mu_x}{\sigma_x^2}\right) = \frac{\frac{\partial G}{\partial x}}{\left|\frac{\partial G}{\partial x}\sigma_x\right|}\frac{x-\mu_x}{\sigma_x} \tag{36}$$

In furtherance of the calculation, a RI should be defined. By definition, RI is the minimum distance from the origin to the failure surface. Coordinates of the point on the failure surface at a distance shortest to the origin can be expressed as:

$$U^* = \beta\cos(\theta_u) \tag{37}$$

where $\cos(\theta_u)$ (or $\cos(\theta_x)$) denotes the direction cosine of the unit outward normal vector (also known as the sensitivity vector (α_x)) and is determined from (Xiao et al., 2011; Guo and Du, 2009):

$$\cos(\theta_x) = \alpha_x = -\frac{\frac{\partial G}{\partial x}\sigma_x}{\left|\frac{\partial G}{\partial x}\sigma_x\right|} \tag{38}$$

Substituting Eq. (38) into Eq. (37), U^* is calculated as:

$$U^* = -\beta\frac{\frac{\partial G}{\partial x}\sigma_x}{\left|\frac{\partial G}{\partial x}\sigma_x\right|} \tag{39}$$

Now, if the term $\frac{(x-\mu_x)}{\sigma_x}$ in Eq. (36) is replaced by U^*, Eq. (40) is obtained:

$$\frac{\partial\beta}{\partial\sigma_x} = \frac{\frac{\partial G}{\partial x}}{\left|\frac{\partial G}{\partial x}\sigma_x\right|} \times \left(-\beta\frac{\frac{\partial G}{\partial x}\sigma_x}{\left|\frac{\partial G}{\partial x}\sigma_x\right|}\right) = \frac{\left(\frac{\partial G}{\partial x}\right)^2\sigma_x}{\left|\frac{\partial G}{\partial x}\sigma_x\right|^2}\beta \tag{40}$$

The reliability sensitivities with respect to the mean and standard deviations, $\frac{\partial\beta}{\partial\mu_x}$, and $\frac{\partial\beta}{\partial\sigma_x}$ are used interchangeably as dBeta/dMu and dBeta/dSigma, respectively in the rest of this paper. Sensitivities of failure probability with respect to the mean and standard deviations.

$\frac{\partial P_f}{\partial\mu_x}$, and $\frac{\partial P_f}{\partial\sigma_x}$ (or dPf/dMu and dPf/dSigma) of the variables involved can be calculated according to Eq. (26).

The above is used in developing an algorithm coded in MATLAB, which is developed for the purpose of this study. Initially, in the stochastic parametric FEA model, the loads were applied to the structure in an uncoupled way ignoring fluid-structure interactions, and the environmental parameters were used in evaluating the magnitude and distribution of the loads. In the present study, these parameters are reintroduced into the stochastic model and the equations incorporated in the LSF sub-routine model of the FORM on implementation of the SSA.

The algorithm used in (Far and Huang, 2019) employed the Advanced First Order Second Moment Method (AFOSM), which have a number of limitations, such as not being suitable for nonlinear limit states. To address this problem, the iterative FORM algorithm (successfully validated against the literature (Shittu et al., 2020a)) has been incorporated into the SSA in this study. Better beta index, as well as sensitivity estimates, were obtained, which offers another solution to a drawback of the AFOSM.

4.4. Stochastic variables

The nine (9) stochastic variables considered in this study are presented in Table 4. The coefficient of variation (CoV) of all stochastic variables was assumed to vary from 0.02 to 0.2 by a step increase of 0.02 (V) Det Norske Veritas. (1992) except for the variables having Weibull distribution (Shittu et al., 2020a). The CoV values were chosen based on guidance specified in design standards, among other sources such as (Shittu et al., 2020a; Velarde et al., 2019; V) Det Norske Veritas. (1992). The OWT support structure is very large and thus will exhibit nonlinearity as it is exposed to high dynamic loads. Thus, to cover for such inherent uncertainties, there is a need to assume appropriate uncertainties derived from (Shittu et al., 2020a, 2020b, 2021a; Shittu, 2020; Kolios and Wang, 2018; Ivanhoe et al., 2020; Kolios, 2010; Al-Sanad et al., 2021), which were measured in terms of the CoVs as adopted in this study.

4.5. FORM (first order reliability method)

Having obtained the performance function from regression, the FORM is used to calculate the RI β. The FORM Hasofer Lind Rackwitz Fiessler (HL-RF) algorithm as established in (Shittu et al., 2020a, 2020b, 2021a, 2021b; Shittu, 2020; Hasofer and Lind, 1974) is applied in this paper.

5. Results and discussion

A key output of the SSA is a set of failure probabilities and reliability indices for the analysed limit states. In this section, SSA of the OWT support structure was performed, and the effect of the structural response on the RI as the CoV is varied is studied and depicted in Fig. 6(a–e). It can be inferred that higher safety indices were recorded for the buckling and deformation limit states. The RI varied considerably for the vibration limit state, which is an indication that variability in the uncertainties has a drastic influence on the safety index. While for the fatigue and deformation limit states, the RI varied slightly and hence, an indication that variability in CoV has no drastic influence on the safety index (i.e., compared to the other limit states).

The reliability sensitivities based on the hyper-plane under different variation coefficients are depicted in Fig. 7–16. From the results in each Figure, it can be inferred that the reliability sensitivity of each random variable is sensitive to its distribution parameters and the sensitivities between variables are comparable. The reliability sensitivity is applied in determining the rate of change in the reliability or failure probability due to changes in the variables, such as means and standard deviations, of distributions. The dimensionless sensitivities were computed to investigate the degree of influence of the mean and standard deviation values for each stochastic variable on the reliability of the structure (Far and Huang, 2019; Xiao et al., 2011). Note that Fig. 7–16 each depicts sensitivities of: (a) RI, beta (β)/POF (P_f) to parameter means (μ) (b) RI, beta/POF (P_f) to parameter standard deviations (σ) for the stress, buckling, fatigue, deformation, and vibration limit states and their

Table 4
Stochastic variables.

Description	Mean		Distribution types (Shittu et al., 2020a; Teixeira et al., 2019; Wang et al., 2017; V) Det Norske Veritas. (1992); Horn and Leira (2019); N 1990 Eurocode:, 2002)
	Ultimate load case	Fatigue load case	
Wind speed, V (m/s)	55	20	Weibull
Tilting moment, M_{Tilt} (kN.m)	38,567	3687	Normal
Torsional moment, $M_{Torsion}$ (kN.m)	7876	3483	Normal
Significant wave height, H (m)	17.48	9.4	Weibull
Young's modulus of soil stratum 1, E_{s1} (MPa)	30		Normal
Young's modulus of soil stratum 2, E_{s2} (MPa)	50		
Young's modulus of soil stratum 3, E_{s3} (MPa)	80		
RNA Weight, W_{RNA} (kg)	1,072,000		Normal
Peak wave period, T (s)	10.8 14		Lognormal

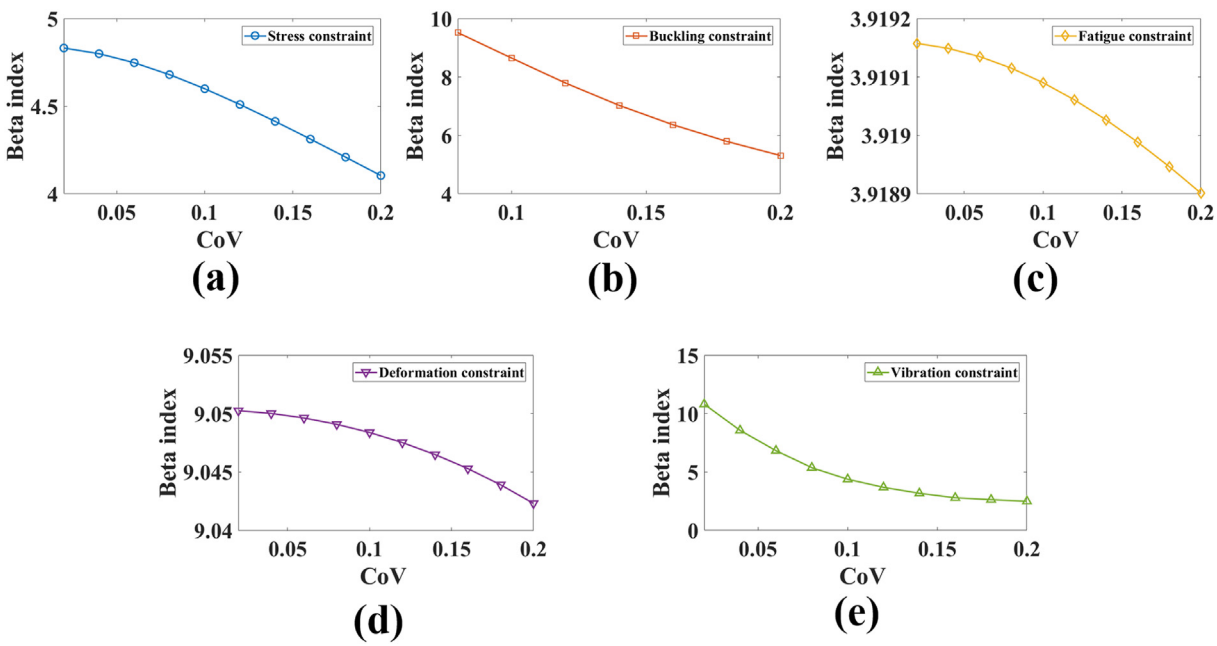

Fig. 6. Variation of the reliability indices with CoV: (a) stress (b) buckling (c) fatigue (design life = 24 years), (d) deformation (e) vibration limit state.

variation with CoV, respectively.

In Figs. 7(a) and 8(a), considering the stress limit state, the order of magnitude of sensitivities with respect to change in mean values, from highest to the lowest are as follows: V, H, T, $M_{Torsional}$, E_{Soil1}, W_{RNA}, M_{Tilt}, E_{Soil2}, and E_{Soil3}. While in Figs. 7(b) and 8(b), which is with respect to change in standard deviation, are as follows: V, T, H, $M_{Torsional}$, E_{Soil1}, M_{Tilt}, W_{RNA}, E_{Soil2}, and E_{Soil3}. From Fig. 9(a) and Fig. 10(a), considering the buckling limit state, the order of magnitude of sensitivities with respect to change in mean values, from highest to the lowest are as follows: V, H, T, W_{RNA}, $M_{Torsional}$, E_{Soil1}, E_{Soil3}, M_{Tilt}, and E_{Soil2}. While in Figs. 9(b) and 10(b), which is with respect to change in standard deviation, are as follows: V, H, T, W_{RNA}, $M_{Torsional}$, E_{Soil1}, E_{Soil3}, M_{Tilt}, and E_{Soil2}. From Figs. 11(a) and 12(a) considering the fatigue limit state, the order of magnitude of sensitivities with respect to change in mean values, are as follows: V, H, T, W_{RNA}, M_{Tilt}, $M_{Torsional}$, E_{Soil2}, E_{Soil1}, and E_{Soil3}. While for Figs. 11(b) and 12(b), which is with respect to change in standard deviation, are as follows: V, T, W_{RNA}, H, M_{Tilt}, $M_{Torsional}$, E_{Soil2}, E_{Soil3}, and E_{Soil1}. From the foregoing, it can be inferred that the variable V, the wind speed, is more sensitive than the other variables in the system considering the stress and buckling (ULS), as well as the Fatigue Limit State (FLS). As can be observed, for the ULS and FLS, the significant wave height and period are, in addition to the wind speed, the main driving factors. In other words, the uncertainties in the hydrodynamic load effects are only secondary compared to the wind load effect. Therefore, in reliability-based design for the ULS and FLS, we need to pay more attention to V than other variables.

Furthermore, in Fig. 13(a) and Fig. 14(a), for the deformation limit state, the order of magnitude of sensitivities with respect to the change in mean values are as follows: V, H, T, M_{Tors} W_{RNA}, M_{Tilt}, E_{Soil1}, E_{Soil2}, and E_{Soil3}. While from Figs. 13(b) and 14(b), which is with respect to change in deviation are as follows: T, V, H M_{Tors}, W_{RNA}, M_{Tilt}, E_{Soil1}, E_{Soil2}, and E_{Soil3}. From Fig. 15(a) and Fig. 16(a), considering the vibration limit state, the order of magnitude of sensitivities with respect to change in mean values, are as follows: V, H, T, W_{Self}, $M_{Torsional}$, E_{Soil1}, E_{Soil2}, M_{Tilt}, and E_{Soil3}. While in

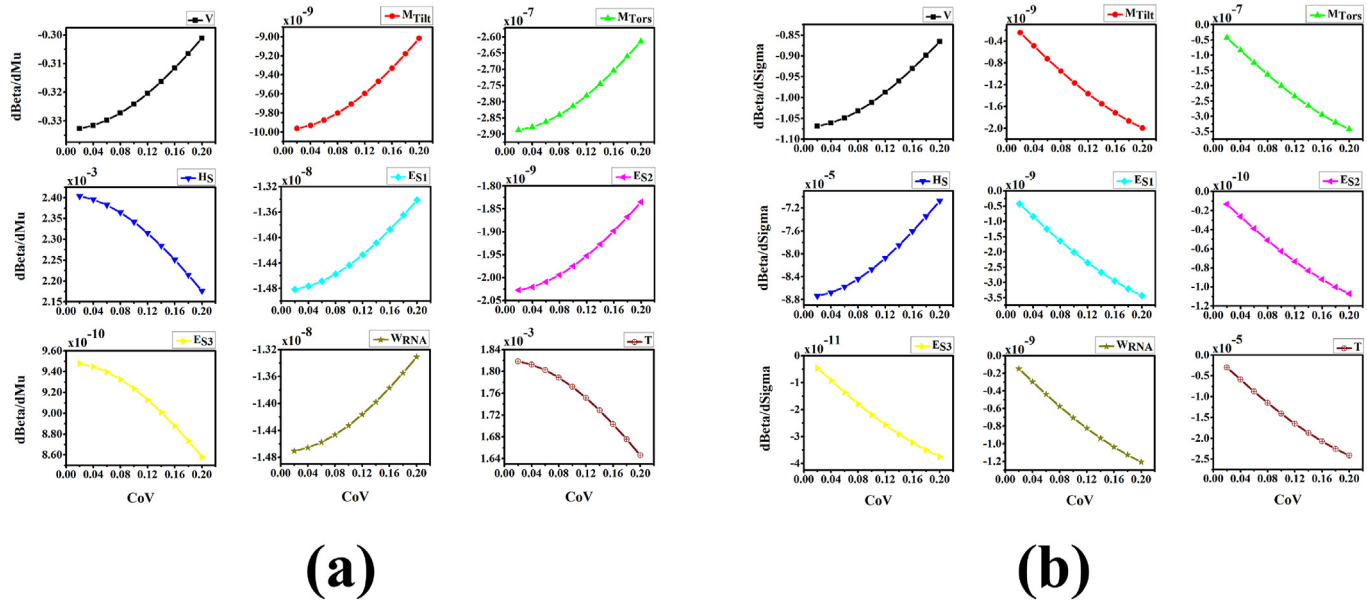

Fig. 7. Sensitivities of parameter means and standard deviations with different coefficients of variation for the stress limit state.

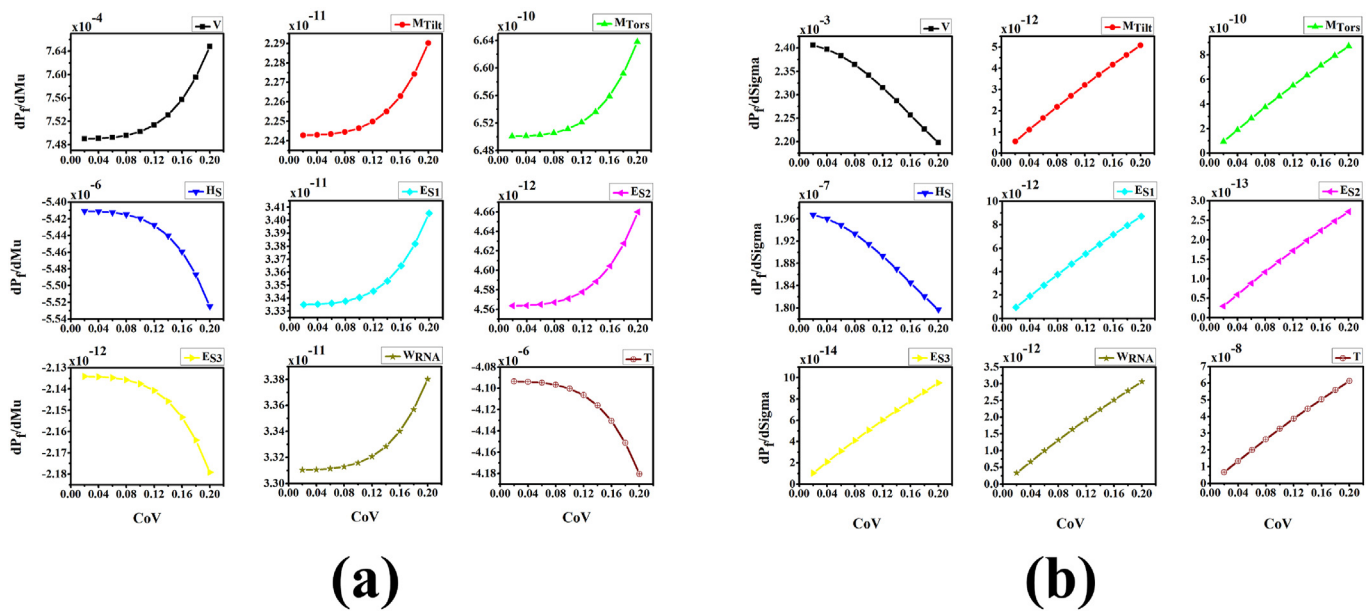

Fig. 8. Sensitivities of parameter means and standard deviations with different coefficients of variation for the stress limit state.

Figs. 15(b) and 16(b), which is with respect to change in deviation, are as follows: H, V, T, W_{Self}, $M_{Torsional}$, E_{Soil1}, E_{Soil2}, M_{Tilt}, and E_{Soil3}. From the foregoing, it can be inferred that there are inconsistencies in the order of magnitude of the system reliability sensitivities for the different cases (i.e. in $\frac{\partial\beta}{\partial\mu}$, and $\frac{\partial\beta}{\partial\sigma}$) considering each limit states. Hence, the stochastic variable with the highest impact cannot be clearly distinguished from the rest. However, V, T, and H, which are hydrodynamic and wind parameters are dominant and are therefore considered as the key stochastic variables in reliability-based design optimisation of the system considering the SLS criteria.

The percentage influence of each structural design variables on the reliability corresponding to the limit states considered, is presented in Tables 5–9.

The sensitivity analyses can be used to improve estimated reliability by identifying the variables that their CoV have the most significant influence on estimated reliability. The estimated reliability is enhanced by reducing the epistemic uncertainty of those variables through, i.e. collecting more data to enable choosing

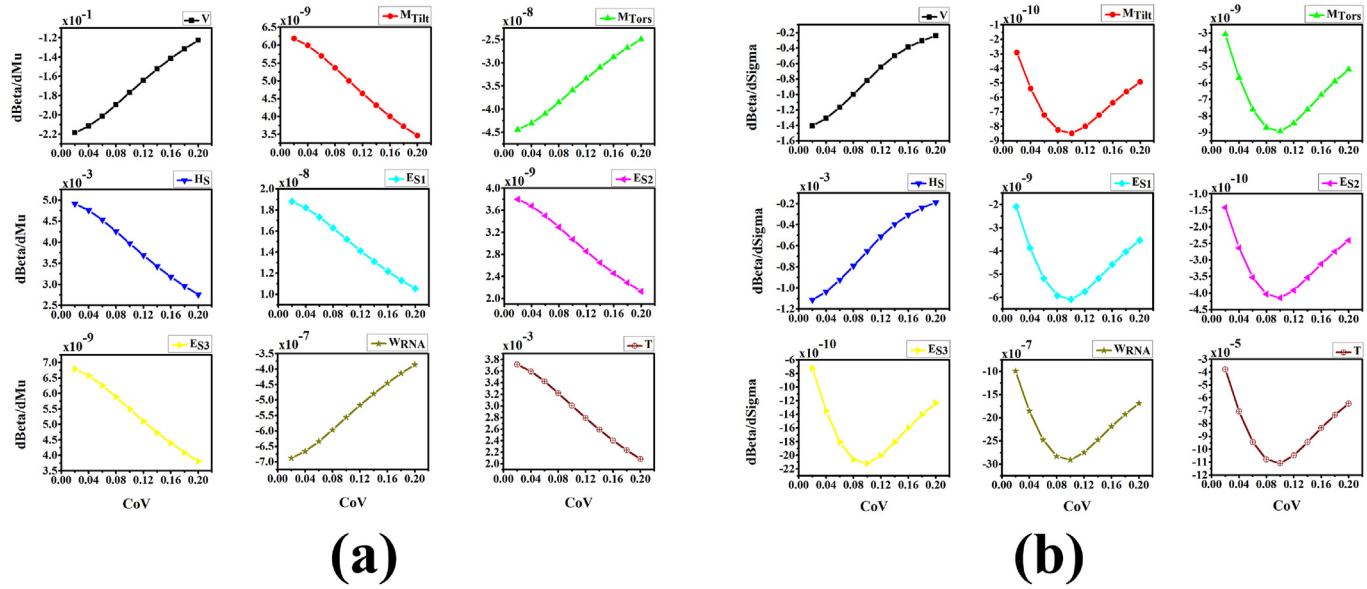

Fig. 9. Sensitivities of parameter means and standard deviations with different coefficients of variation for the buckling limit state.

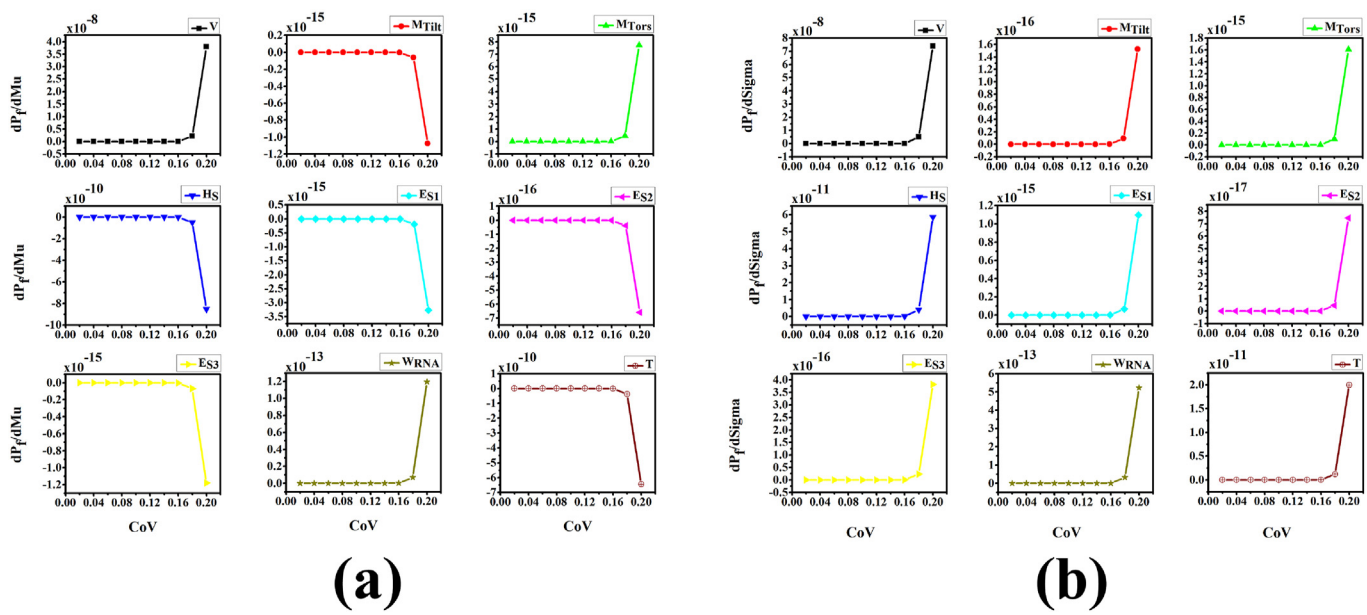

Fig. 10. Sensitivities of parameter means and standard deviations with different coefficients of variation for the buckling limit state.

appropriate probability distribution which better estimates the variables, and in turn lead to a reduction in the values of standard deviation or CoV. In other words, it is crucial to collect appropriate information for wind variation across the site. This should account for the performance of each unit (including factors such as wake effects) as this can significantly alter performance and reliability across the wind farm. For instance, from Fig. 10, and Fig. 16, the POF sensitivities recorded a spike in values as the CoV tend towards higher magnitudes. These behaviours show that the offshore structure studied herein is non-linear, a typical characteristic of complex structures. This further supports the claim that emphases should be laid on acquiring highly accurate data on such structures in order to reduce the inherent uncertainties.

Additionally, a case study is performed to investigate the effects of correlation between the structural design stochastic variables on the reliability indices of the different limit states considered. The variables considered as correlated are the wind speed, tilting moment and torsional moment, and the significant wave height and peak wave period. The calculated reliability indices for the different limit states as they vary with the variation in percentage

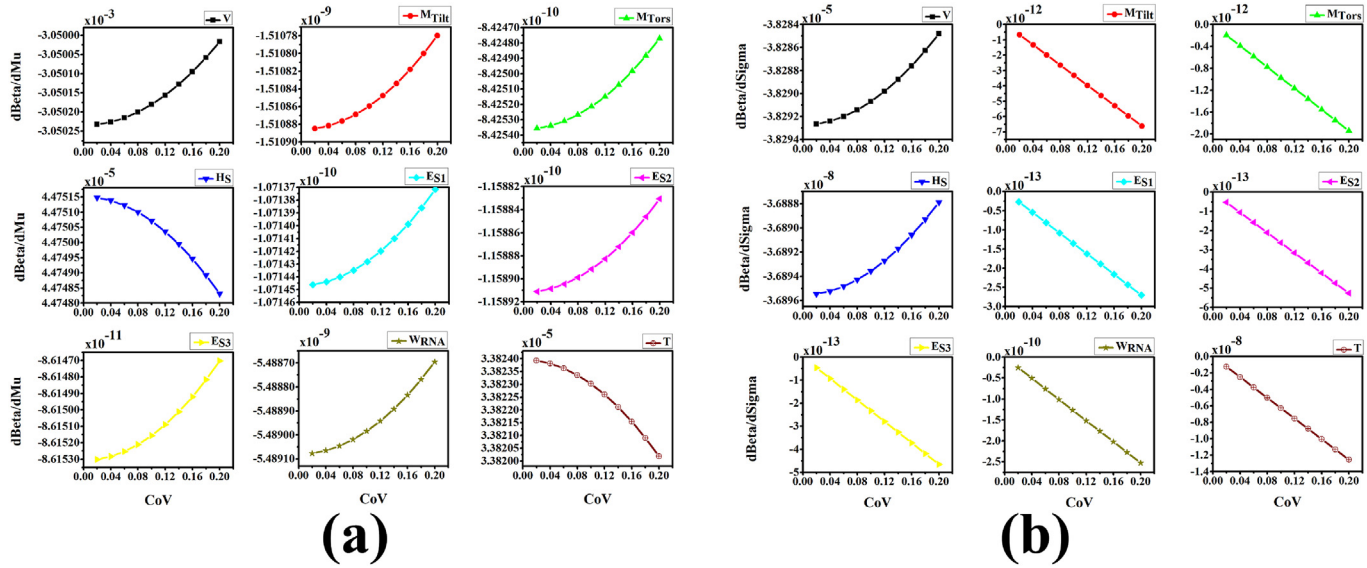

Fig. 11. Sensitivities of parameter means and standard deviations with different coefficients of variation for the fatigue limit state.

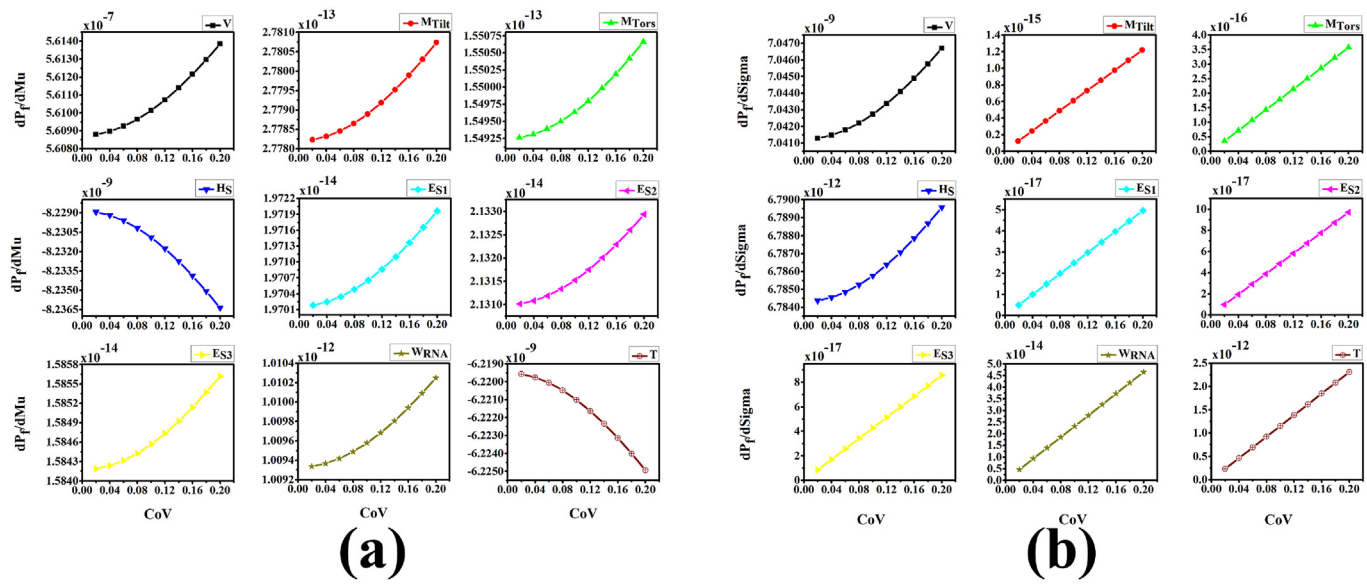

Fig. 12. Sensitivities of parameter means and standard deviations with different coefficients of variation for the fatigue limit state.

correlation (0–90%) is depicted in Fig. 17(a–e). As can be observed, as the correlation between the wind parameters as well as between the hydrodynamic parameters increases the reliability indices calculated decreases. Also, the RI is sensitive to the percentage correlation, and the ULS is calculated to be the highest. Therefore, during structural design for the ULS, the correlation between the different variables should be taken into account. The percentage correlation computation concept as applied in this study was derived from other studies such as in Refs (Shittu, 2020; Melchers, 1999; Ditlevsen and Madsen, 1996; Nowak and Collins, 2012; Shittu et al., 2021a, 2021b). where the underlining principles were illustrated in great detail. Interactive effects between random variables on the reliability sensitivity levels for the OWT support structure can be derived from correlation coefficient equations described in classical reliability engineering textbooks (Ayyub and McCuen, 2011; Choi et al., 2006).

The SSA framework developed will be an invaluable tool for designers with respect to reliability-based design optimisation. This will enable researchers to focus on the parameters with uncertainties having a significant impact on the reliability and assume

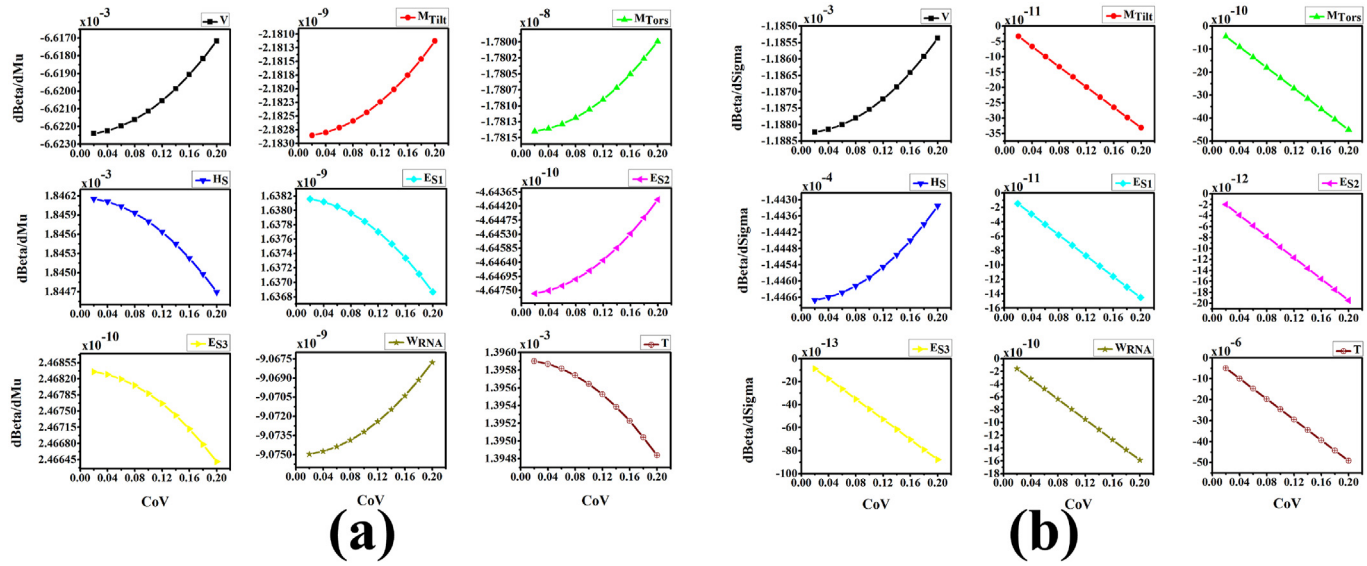

Fig. 13. Sensitivities of parameter means and standard deviations with different coefficients of variation for the deformation limit state.

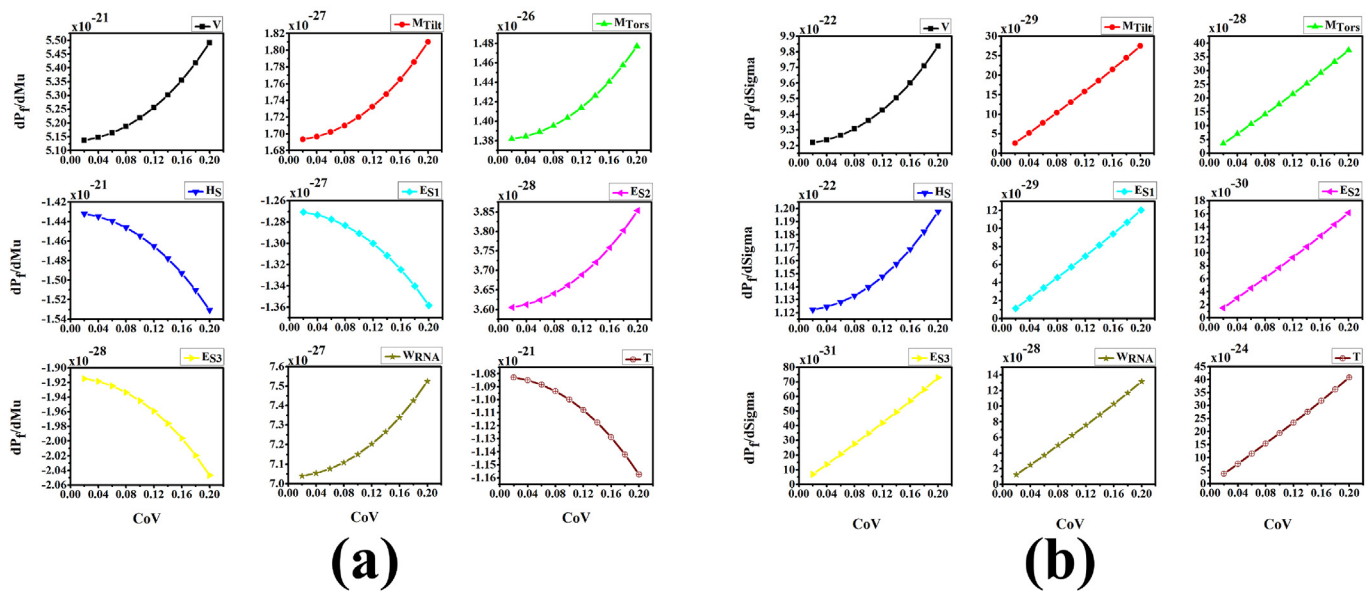

Fig. 14. Sensitivities of parameter means and standard deviations with different coefficients of variation for the deformation limit state.

deterministic values for those having negligible influence. Offshore wind industry practitioners can harness the capability of the framework developed to address the problem of optimising the CAPEX to OPEX ratio which is an issue of priority and hence allows cost reduction activities needed to ensure structural safety and efficient performance of the OWT foundation.

The developed model has an advantage of being easy to use since it employs the well-established FORM unlike methods based on the MCS, which required prohibitively large computational resources to calculate very small values of failure probabilities for complex structures as encountered in this study. Also, it can be applied to problems of implicit performance function (i.e. requiring FEA methods to solve such cases accurately). It should be noted; however, that aero-servo-elastic codes such as GH BLADED, OpenFAST, FLEX5 and HAWC2 which are well-suited options to capture the most important non-linear contributions and enable coupling of the blade and generator with the support structure thereby accounting accurately for fluid-structure interaction as established in (Velarde et al., 2019; Morató et al., 2017, 2019; Ziegler and Muskulus, 2016; Robertson et al., 2019; Hübler et al., 2017; Jiang

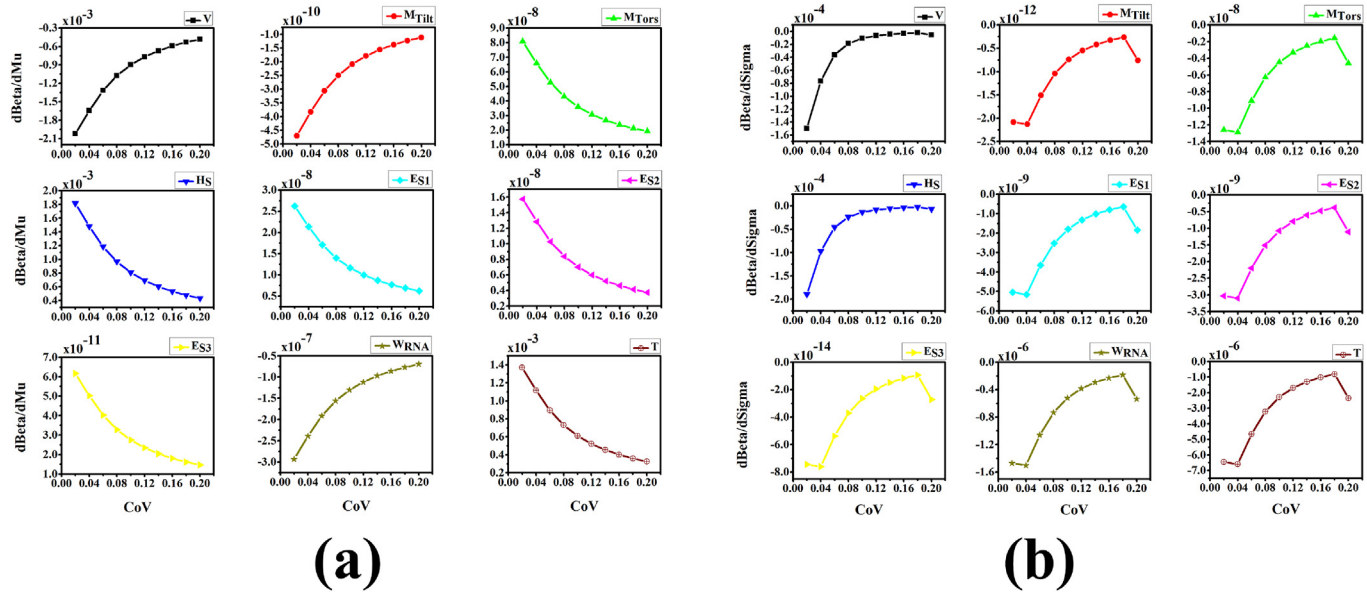

Fig. 15. Sensitivities of parameter means and standard deviations with different coefficients of variation for the vibration limit state.

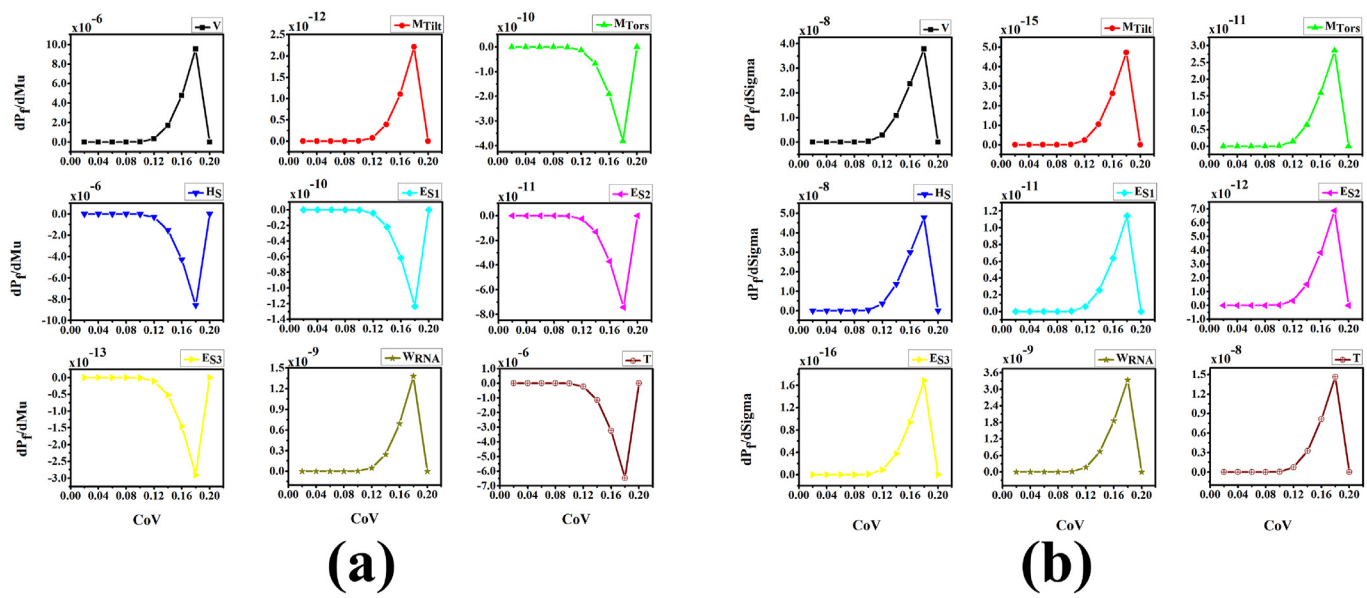

Fig. 16. Sensitivities of parameter means and standard deviations with different coefficients of variation for the vibration limit state.

Table 5
Percentage (%) influence of structural design parameters on reliability corresponding to the stress limit state.

Variables	$\frac{d\beta}{d\mu}$	$\frac{d\beta}{d\sigma}$	$\frac{dP_f}{d\mu}$	$\frac{dP_f}{d\sigma}$
V	9.87E+01	1.00E+02	9.87E+01	1.00E+02
M_{Tilt}	2.96E-06	8.51E-07	2.96E-06	1.26E-06
M_{Tors}	8.57E-05	1.46E-04	8.57E-05	2.16E-04
H_s	7.13E-01	8.17E-03	7.13E-01	4.91E-03
E_{S1}	4.40E-06	1.46E-06	4.40E-06	2.16E-06
E_{S2}	6.01E-07	4.56E-08	6.02E-07	6.75E-08
E_{S3}	2.81E-07	1.60E-08	2.81E-07	2.36E-08
W_{RNA}	4.36E-06	5.14E-07	4.36E-06	7.60E-07
T	5.39E-01	1.03E-02	5.43E-01	1.52E-02

Table 6
Percentage (%) influence of structural design parameters on reliability corresponding to the buckling limit state.

Variables	$\frac{d\beta}{d\mu}$	$\frac{d\beta}{d\sigma}$	$\frac{dP_f}{d\mu}$	$\frac{dP_f}{d\sigma}$
V	9.62E+01	9.99E+01	9.62E+01	9.99E+01
M_{Tilt}	2.72E-06	5.20E-09	2.72E-06	2.05E-07
M_{Tors}	1.96E-05	5.48E-08	1.96E-05	2.16E-06
H_s	2.16E+00	7.91E-02	2.16E+00	7.91E-02
E_{S1}	8.28E-06	3.73E-08	8.28E-06	1.47E-06
E_{S2}	1.67E-06	2.54E-09	1.67E-06	1.00E-07
E_{S3}	2.99E-06	1.30E-08	2.99E-06	5.12E-07
W_{RNA}	3.03E-04	1.78E-05	3.03E-04	7.03E-04
T	1.64E+00	6.80E-04	1.64E+00	2.68E-02

Table 7
Percentage (%) influence of structural design parameters on reliability corresponding to the fatigue limits state.

Variables	$\frac{d\beta}{d\mu}$	$\frac{d\beta}{d\sigma}$	$\frac{dP_f}{d\mu}$	$\frac{dP_f}{d\sigma}$
V	9.69E+01	4.06E+01	9.75E+01	7.20E+01
M_{Tilt}	4.70E-05	3.07E-02	4.84E-05	1.44E-02
M_{Tors}	2.63E-05	9.00E-03	2.70E-05	4.23E-03
H_s	1.42E+00	3.91E-02	1.43E+00	6.94E-02
E_{S1}	3.34E-06	1.25E-03	3.43E-06	5.87E-04
E_{S2}	3.61E-06	2.44E-03	3.71E-06	1.15E-03
E_{S3}	2.68E-06	2.16E-03	2.76E-06	1.01E-03
W_{RNA}	1.71E-04	1.17E+00	1.76E-04	5.50E-01
T	1.68E+00	5.82E+01	1.03E+00	2.73E+01

Table 8
Percentage (%) influence of structural design parameters on reliability corresponding to the deformation limit state.

Variables	$\frac{d\beta}{d\mu}$	$\frac{d\beta}{d\sigma}$	$\frac{dP_f}{d\mu}$	$\frac{dP_f}{d\sigma}$
V	6.75E+01	6.01E+00	6.71E+01	5.80E+01
M_{Tilt}	2.22E-05	6.29E-04	2.21E-05	2.35E-04
M_{Tors}	1.81E-04	8.55E-03	1.81E-04	3.20E-03
H_s	1.88E+01	7.32E-01	1.87E+01	7.07E+00
E_{S1}	1.67E-05	2.75E-04	1.66E-05	1.03E-04
E_{S2}	4.73E-06	3.69E-05	4.71E-06	1.38E-05
E_{S3}	2.51E-06	1.67E-05	2.50E-06	6.23E-06
W_{RNA}	9.25E-05	3.01E-03	9.20E-05	1.13E-03
T	1.37E+01	9.32E+01	1.42E+01	3.49E+01

Table 9
Percentage (%) influence of structural design parameters on reliability corresponding to the vibration limit state.

Variables	$\frac{d\beta}{d\mu}$	$\frac{d\beta}{d\sigma}$	$\frac{dP_f}{d\mu}$	$\frac{dP_f}{d\sigma}$
V	3.88E+01	4.30E+01	3.88E+01	3.68E+01
M_{Tilt}	9.02E-06	6.96E-07	9.02E-06	4.37E-06
M_{Tors}	1.55E-03	4.21E-03	1.55E-03	2.64E-02
H_s	3.49E+01	5.44E+01	3.49E+01	4.65E+01
E_{S1}	5.03E-04	1.68E-03	5.03E-04	1.06E-02
E_{S2}	3.02E-04	1.01E-03	3.02E-04	6.36E-03
E_{S3}	1.18E-06	2.48E-08	1.18E-06	1.56E-07
W_{Self}	5.62E-03	4.91E-01	5.62E-03	3.08E+00
T	2.63E+01	2.15E+00	2.63E+01	1.35E+01

et al., 2017) is recommended for future study. Also, limitations to the developed approach, which is an approximation method rather than an exact solution and may lead to loss of information and restrict the domain of stochastic variables are identified. According to (Velarde et al., 2019), for non-linear models involving a large domain of stochastic variables, the sensitivity measured at a specific reference point whilst using the derivative-based approach may be invalid over the entire input space. Problems of too highly non-linear performance functions may result in inaccurate results since the more the nonlinearity of an LSF the larger the errors will be.

6. Conclusion

This paper presented a methodology for the sensitivity assessment of the inherent stochastic variables often imposed on typical complex OWT support structures due to harsh environments. Sensitivity refers to the most critical variables that can radically impact on the reliability performance of the structure. The reliability of the structure can be improved by reducing the uncertainties by virtue of statistical parameters for the structural design variables having an insignificant impact on the reliability. The proposed method was used to investigate the influence of several stochastic variables on the reliability of the structure. This proposed non-intrusive method involves a sequence of steps that incorporates responses obtained from parametric FEA with the iterative FORM-based SSA via multivariate quadratic polynomial regression for the approximation of more reliable levels of sensitivities with respect to the various stochastic variables. The SSA adopts an approach that determines the search direction based on function gradients.

For the ULS, the most sensitive variable, the wind speed, V is 94% more sensitive than the second most influencing variable, the wave height, H_s considering reliability sensitivities with respect to the mean, and 99% considering reliability sensitivities with respect to standard deviation. For the FLS, the most sensitive variable, V is 95% more sensitive than the second, T considering the reliability sensitivities to the mean, and 45% considering reliability sensitivities to the standard deviations. While for the SLS, the most sensitive variable, V is 49% higher than the second, hydrodynamic effects considering reliability sensitivities to the mean, and the most, the hydrodynamic effects higher than V with 33% considering reliability sensitivities to standard deviation.

In this study, it is revealed that the key structural design variables to be considered for Reliability-Based Design Optimisation (RBDO) are the wind speed, significant wave height and peak wave period for all design limit states studied. Moreover, it can be concluded that the influence of weight, torsional moments resulting from aerodynamic loads as well as that of soil-structure interactions of the first soil strata is not insignificant for all the considered limit states. The influence of the other structural design variables considered stochastic in this study: the significance of uncertainties in the second and third soil strata, as well as the tilting moment, can be considered negligible. Also, the study ascertained how important the correlation between structural design variables is to the reliability of the OWT support structure.

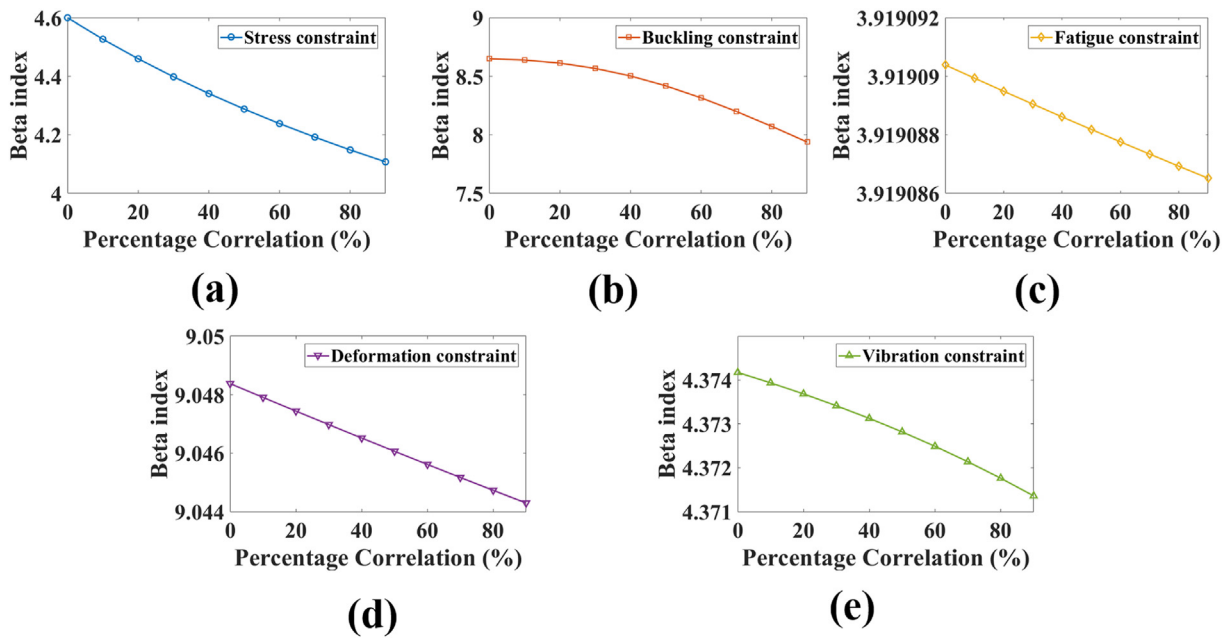

Fig. 17. Variation of reliability indices with change in percentage correlation for: (a) the stress (b) buckling (c) fatigue (d) deformation (e) vibration limit states.

Declaration of competing interest

The authors declare that they have no known competing financial interests or personal relationships that could have appeared to influence the work reported in this paper.

Acknowledgements

Author Abdulhakim A. Shittu would like to acknowledge the Petroleum Technology Development Fund (PTDF), Nigeria, for doctoral study scholarship, award number: PTDF/ED/PHD/SAA/1142/17.

References

DNV. DNV-OS-, May. 2014. J101 Design of Offshore Wind Turbine Structures, pp. 212–214. May.

IEC. IEC 61400-1, 2005. Wind Turbines Part 1: Design Requirements.

Achmus, M., Abdel-Rahman, K., 2005. Finite element modelling of horizontally loaded monopile foundations for offshore wind energy converters in Germany. Front. Offshore Geotech. https://doi.org/10.1201/NOE0415390637.ch38 (August 2005). Available at:

Al-Sanad, S., Wang, L., Parol, J., Kolios, A., April 2021. Reliability-based Design Optimisation Framework for Wind Turbine Towers, vol. 167. Renewable Energy. Elsevier Ltd, pp. 942–953. https://doi.org/10.1016/j.renene.2020.12.022. Available at: DOI:

Ayyub, B.M., McCuen, R.H., 2011. Probability, Statistics, and Reliability for Engineers and Scientists, Third. Taylor and Francis Group, Boca Raton, FL, USA.

Breitung, K., 1984. Asymptotic approximations for multinormal integrals. J. Eng. Mech. 110 (3), 357–366.

Choi, S.-K., Grandhi, R., Canfield, R., 2006. Reliability-Based Structural Design. Springer, USA.

Coccon, M.N., Song, J., Ok, S.Y., Galvanetto, U., 2017. A new approach to system reliability analysis of offshore structures using dominant failure modes identified by selective searching technique. KSCE J. Civil Eng. 21 (6), 2360–2372. https://doi.org/10.1007/s12205-016-1192-z. Available at:

Damiani, R., Song, H., 2013. A jacket sizing tool for offshore wind turbines within the systems engineering initiative. Houston, Texas, USA. In: Offshore Technology Conference, OTC 24140. https://doi.org/10.4043/24140-MS. Available at:

Damiani, R.R., Song, H., Robertson, A.N., Jonkman, J.M., 2013. Assessing the importance of nonlinearities in the development of a substructure model for the wind turbine CAE tool FAST. Ocean Renew. Energy ume 8. https://doi.org/10.1115/OMAE2013-11434, 8(March): V008T09A093. Available at:

Det Norske Veritas, 2000. Environmental Conditions and Environmental Loads. DNV RP C205.

Ditlevsen, O., Madsen, H.O., 1996. Structural Reliability Methods. Wiley, New York.

DNV, G.L.A.S., 2016. DNVGL-ST-0126 : Support Structures for Wind Turbines. DNV GL - Standard Høvik. Det Norske Veritas, Norway, p. 182. https://doi.org/10.1016/j.jbiomech.2014.11.025. Available at:

DNV, G.L.A.S., 2016. DNVGL-ST-0437: Loads and Site Conditions for Wind Turbines. DNV GL - Standard. Det Norske Veritas, Høvik, Norway, p. 108.

Far, M.S., Huang, H., 2019. Simplified algorithm for reliability sensitivity analysis of structures: a spreadsheet implementation. PLoS One 14 (3), 1–22. https://doi.org/10.1371/journal.pone.0213199. Available at:

Fisher, T., De Vries, W., Schmidt, B., 2010. Upwind Design Basis (WP4 Offshore Foundations and Support Structures). Project Upwind Contract No. 019945. SES6. https://doi.org/10.1016/S0140-6736(02)81074-1. Available at:

Freebury, G., Musial, W., 2000. Determining equivalent damage loading for full-scale wind turbine blade fatigue tests. In: 2000 ASME Wind Energy Symposium. https://doi.org/10.2514/6.2000-50 (February). Available at:

Gentils, T., Wang, L., Kolios, A., 2017. Integrated Structural Optimisation of Offshore Wind Turbine Support Structures Based on Finite Element Analysis and Genetic Algorithm, vol. 199. Applied Energy. Elsevier Ltd, pp. 187–204. https://doi.org/10.1016/j.apenergy.2017.05.009. Available at:

Guo, J., Du, X., 2009. Reliability sensitivity analysis with random and interval variables. Int. J. Numer. Methods Eng. 78 (1585–1617), 1102–1119. https://doi.org/10.1002/nme.2543. Available at:

Hald, T., Mørch, C., Jensen, L., Bakmar, C.L., Ahle, K., 2009. Revisiting monopile design using py curves. Results from full scale measurements on Horns Rev. In: Proceedings of European Offshore Wind 2009 Conference.

Haldar, A., Mahadevan, S., 1999. Probability, Reliability, and Statistical Methods in Engineering Design. Wiley.

Hasofer, A., Lind, N., 1974. An exact and invariant second moment code format. J. Engrg. Mech. Div ASCE. 100 (1), 111–121.

ANSYS, 2018. ANSYS help documentation.

Horn, J.T., Leira, B.J., November 2019. Fatigue Reliability Assessment of Offshore Wind Turbines with Stochastic availability. Elsevier Ltd Reliability Engineering and System Safety 191. https://doi.org/10.1016/j.ress.2019.106550. Available at:

Huang, X., Li, Y., Zhang, Y., Zhang, X., 2018. A new direct second-order reliability analysis method. Elsevier Inc Appl. Math. Model. 55, 68–80. https://doi.org/10.1016/j.apm.2017.10.026. Available at:

Hübler, C., Gebhardt, C.G., Rolfes, R., October 2017. Hierarchical Four-step Global Sensitivity Analysis of Offshore Wind Turbines Based on Aeroelastic Time Domain Simulations, vol. 111. Renewable Energy. Elsevier Ltd, pp. 878–891. https://doi.org/10.1016/j.renene.2017.05.013. Available at: DOI:

Hyldal, S.P., 2012. Soil-structure Interaction for Non- Slender , Large-Diameter Offshore.

Ivanhoe, R.O., Wang, L., Kolios, A., November 2020. Generic framework for reliability assessment of offshore wind turbine jacket support structures under stochastic and time dependent variables. Elsevier Ltd Ocean Eng. 216, 107691. https://doi.org/10.1016/j.oceaneng.2020.107691. Available at:

JacketSE, Damiani R., 2016. An Offshore Wind Turbine Jacket Sizing Tool Theory Manual and Sample Usage with Preliminary Validation. Denver West Parkway Golden, CO.

Jalbi, S., Bhattacharya, S., 1 December 2020. Concept design of jacket foundations for offshore wind turbines in 10 steps. Elsevier Soil Dynam. Earthq. Eng. 139,

106357. https://doi.org/10.1016/J.SOILDYN.2020.106357. Available at:
Jiang, Z., Hu, W., Dong, W., Gao, Z., Ren, Z., 2017. Structural reliability analysis of wind turbines: a review. Energies 10 (12), 1–25. https://doi.org/10.3390/en10122099. Available at:
Jonkman, J., Butterfield, S., Musial, W., Scott, G., 2009. Definition of a 5-MW Reference Wind Turbine for Offshore System Development. https://doi.org/10.2172/947422 (February). Available at:
Jung, S., Kim, S.R., Patil, A., Hung, L.C., 2015. Effect of monopile foundation modeling on the structural response of a 5-MW offshore wind turbine tower. Elsevier Ocean Eng. 109, 479–488. https://doi.org/10.1016/j.oceaneng.2015.09.033. Available at:
Kala, Z., 2011. Sensitivity analysis of steel plane frames with initial imperfections. Elsevier Ltd Eng. Struct. 33 (8), 2342–2349. https://doi.org/10.1016/j.engstruct.2011.04.007. Available at:
Kang, F., Xu, Q., Li, J., June 2016. Slope reliability analysis using surrogate models via new support vector machines with swarm intelligence. Elsevier Inc. Appl. Math. Model. 40 (11–12), 6105–6120. https://doi.org/10.1016/j.apm.2016.01.050. Available at:
Kolios, A., 2010. A Multi-Configuration Approach to Reliability Based Structural Integrity Assessment for Ultimate Strength. Cranfield University.
Kolios, A., Wang, L., 2018. Advanced Reliability Assessment of Offshore Wind Turbine Monopiles by Combining Reliability Analysis Method and SHM/CM Technology, pp. 1412–1419.
Kolios, A.J., Rodriguez-Tsouroukdissian, A., Salonitis, K., 2016. Multi-criteria decision analysis of offshore wind turbines support structures under stochastic inputs. Taylor & Francis Ships Offshore Struct. 11 (1), 38–49. https://doi.org/10.1080/17445302.2014.961295. Available at:
Kolios, A., Di Maio, L.F., Wang, L., Cui, L., Sheng, Q., 2018. Reliability assessment of point-absorber wave energy converters. Elsevier Ltd Ocean Eng. 163, 40–50. https://doi.org/10.1016/j.oceaneng.2018.05.048. October 2017.
Kühn, M., 1999. Dynamics and Design Optimization of Offshore Wind Energy Conversion Systems. Sciences-, New York.
Kwak, B.M., Lee, Tae Won, 1987. Sensitivity analysis for reliability-based optimization using an AFOSM method. Comput. Struct. 27 (3), 399–406. https://doi.org/10.1016/0045-7949(87)90064-2. Available at:
Lee, Y.S., Choi, B.L., Lee, J.H., Kim, S.Y., Han, S., 2014. Reliability-based Design Optimization of Monopile Transition Piece for Offshore Wind Turbine System, vol. 71. Renewable Energy. Elsevier Ltd, pp. 729–741. https://doi.org/10.1016/j.renene.2014.06.017. Available at:
Leimeister, M., Kolios, A., 2018. A review of reliability-based methods for risk analysis and their application in the offshore wind industry. In: Renewable and Sustainable Energy Reviews. Elsevier Ltd, p. 91. https://doi.org/10.1016/j.rser.2018.04.004 (July 2017): 1065–1076. Available at:
Lu, Z., Song, J., Song, S., Yue, Z., Wang, J., October 2010. Reliability sensitivity by method of moments. Appl. Math. Model. 34 (10), 2860–2871. https://doi.org/10.1016/j.apm.2009.12.020. Available at:
Martin, H., Spano, G., Küster, J.F., Collu, M., Kolios, A.J., 2013. Application and extension of the TOPSIS method for the assessment of floating offshore wind turbine support structures. Ships Offshore Struct. 8 (5), 477–487. https://doi.org/10.1080/17445302.2012.718957. Available at:
Martinez-Luengo, M., Kolios, A., Wang, L., 2017. Parametric FEA modelling of offshore wind turbine support structures: towards scaling-up and CAPEX reduction. Int. J. Mar. Energy 19 (2017), 16–31. https://doi.org/10.1016/j.ijome.2017.05.005. Available at:
Melchers, R.E., 1999. Structural Reliability Analysis and Prediction. John Wiley \\\\& Sons.
Minguez, L., 2015. Fatigue and Fracture Mechanics of Offshore Wind Turbine Support Structures. Cranfield university.
Morató, A., Sriramula, S., Krishnan, N., 2017. Reliability analysis of offshore wind turbine support structures using kriging models. In: Walls, L., Revie, M., Bedford, B. (Eds.), Risk, Reliability and Safety: Innovating Theory and Practice. Didcot. Taylor & Francis Group, London, UK.
Morató, A., Sriramula, S., Krishnan, N., August 2019. Kriging models for aero-elastic simulations and reliability analysis of offshore wind turbine support structures. Taylor and Francis Ltd. Ships Offshore Struct. 14 (6), 545–558. https://doi.org/10.1080/17445302.2018.1522738. Available at:
Muskulus M., Schafhirt S. Design optimization of wind turbine support structures—a review. J. Ocean Wind Energy. 2310; 1(1): 12–22. Available at: DOI:10.13140/RG.2.1.5125.5766.
BSI. BS EN 1990, 2002. Eurocode: Basis of Structural Design. British standard institute.
ANSYS Inc, 2010. Introduction to Contacts - ANSYS Mechanical Structural Nonlinearities. December.
Nowak, A.S., Collins, K.R., 2012. Reliability of Structures, second ed. CRC Press.
Periçaro, G.A., Santos, S.R., Ribeiro, A.A., Matioli, L.C., 2015. HLRF-BFGS optimization algorithm for structural reliability. Elsevier Inc. Appl. Math. Model. 39 (7), 2025–2035. https://doi.org/10.1016/j.apm.2014.10.024. Available at:
Petrini, F., Manenti, S., Gkoumas, K., Bontempi, F., 2010. Structural design and analysis of offshore wind turbines from a system point of view. Wind Eng. 34 (1), 85–107. https://doi.org/10.1260/0309-524X.34.1.85. Available at:
Robertson, A.N., Shaler, K., Sethuraman, L., Jonkman, J., 2019. Sensitivity analysis of the effect of wind characteristics and turbine properties on wind turbine loads. Wind Energy Sci. Copernicus GmbH; Sept. 4 (3), 479–513. https://doi.org/10.5194/wes-4-479-2019. Available at:
Rule, G.L., 1995. For Regulation IV-Non Marine Technology, Part 2 Offshore Wind Energy. Hamburg.
Shittu, A.A., 2020. Structural Reliability Assessment of Complex Offshore Structures Based on Non-intrusive Stochastic Methods. Cranfield University, Bedford, UK.
Shittu, A.A., Mehmanparast, A., Wang, L., Salonitis, K., Kolios, A., 2020a. Comparative study of structural reliability assessment methods for offshore wind turbine jacket support structures. Appl. Sci. MDPI AG 10 (3). https://doi.org/10.3390/app10030860. Available at:
Shittu, A.A., Mehmanparast, A., Shafiee, M., Kolios, A., Hart, P., Pilario, K.E., 2020b. Structural reliability assessment of offshore wind turbine support structures subjected to pitting corrosion-fatigue: a damage tolerance modelling approach. Wind Energy. John Wiley & Sons, Ltd 23 (11), 2004–2026. https://doi.org/10.1002/we.2542. Available at:
Shittu, A.A., Kolios, A., Mehmanparast, A., 2021a. A systematic review of structural reliability methods for deformation and fatigue analysis of offshore jacket structures. Metals 11, 50. https://doi.org/10.3390/MET11010050. Multidisciplinary Digital Publishing Institute; December 2020; 11(1): 50. Available at:
Shittu, A.A., Mehmanparast, A., Hart, P., Kolios, A., 1 November 2021. Comparative study between S-N and fracture mechanics approach on reliability assessment of offshore wind turbine jacket foundations. Elsevier Reliab. Eng. Syst. Saf. 215, 107838. https://doi.org/10.1016/J.RESS.2021.107838. Available at:
Teixeira, R., O'Connor, A., Nogal, M., 2019. Probabilistic Sensitivity Analysis of Offshore Wind Turbines Using a Transformed Kullback-Leibler Divergence. Structural Safety. Elsevier B.V., p. 81. https://doi.org/10.1016/j.strusafe.2019.03.007. Available at:
(DNV) Det Norske Veritas, 1992. Structural reliability analysis of marine structures. DNV CN 30-6.
(DNV) Det Norske Veritas, 2005. Fatigue Design of Offshore Steel Structures. Recommended Practice DNV-RPC203, p. 126 (October).
Velarde, J., Kramhøft, C., Sørensen, J.D., 2019. Global Sensitivity Analysis of Offshore Wind Turbine Foundation Fatigue Loads, vol. 140. Renewable Energy. Elsevier Ltd, pp. 177–189. https://doi.org/10.1016/j.renene.2019.03.055. Available at:
Wang, L., Liu, X., Renevier, N., Stables, M., Hall, G.M., 2014. Nonlinear Aeroelastic Modelling for Wind Turbine Blades Based on Blade Element Momentum Theory and Geometrically Exact Beam Theory, vol. 76. Energy. Elsevier Ltd, pp. 487–501. https://doi.org/10.1016/j.energy.2014.08.046. Available at:
Wang, L., Kolios, A., Delafin, P.-L., Nishino, T., Bird, T., 2015. Fluid structure interaction modelling of a novel 10MW vertical-axis wind turbine rotor based on computational fluid dynamics and finite element analysis. In: EWEA 2015 - Scientific Proceedings, vol. 44. European Wind Energy Association Annual Conference and Exhibition 2015 (0).
Wang, L., Kolios, A., Nishino, T., Delafin, P.L., Bird, T., 2016a. Structural optimisation of vertical-axis wind turbine composite blades based on finite element analysis and genetic algorithm. Elsevier Ltd Compos. Struct. 153, 123–138. https://doi.org/10.1016/j.compstruct.2016.06.003. January 2015.
Wang, L., Quant, R., Kolios, A., 2016b. Fluid structure interaction modelling of horizontal-axis wind turbine blades based on CFD and FEA. Elsevier J. Wind Eng. Ind. Aerod. 158, 11–25. https://doi.org/10.1016/j.jweia.2016.09.006. Available at: DOI:
Wang, L., Kolios, A., 2017. A generic framework for reliability assessment of offshore wind turbine monopiles. In: Guedes Soares, C., Garbatov, Y. (Eds.), Progress in the Analysis and Design of Marine Structures - Proceedings of the 6th International Conference on Marine Structures, MARSTRUCT 2017. Taylor and Francis Group, Lisbon, Portugal, pp. 931–938. https://doi.org/10.1201/9781315157368-105. Available at:
Wind, I.E.C., 2009. Turbines - Part 3: Design Requirements for Offshore Wind Turbines. IEC 61400-3. Geneva, Switzerland.
Xiao, N.C., Huang, H.Z., Wang, Z., Pang, Y., He, L., 2011. Reliability sensitivity analysis for structural systems in interval probability form. Struct. Multidiscip. Optim. 44 (5), 691–705. https://doi.org/10.1007/s00158-011-0652-9. Available at:
Zhang, L., Lu, Z., Wang, P., 2015. Efficient structural reliability analysis method based on advanced Kriging model. Elsevier Inc. Appl. Math. Model. 39 (2), 781–793. https://doi.org/10.1016/j.apm.2014.07.008. Available at:
Zhao, H., Li, S., Ru, Z., April 2017. Adaptive reliability analysis based on a support vector machine and its application to rock engineering. Elsevier Inc. Appl. Math. Model. 44, 508–522. https://doi.org/10.1016/j.apm.2017.02.020. Available at:
Ziegler, L., Muskulus, M., 2016. Fatigue reassessment for lifetime extension of offshore wind monopile substructures. In: Journal of Physics: Conference Series. Institute of Physics Publishing, p. 92010. https://doi.org/10.1088/1742-6596/753/9/092010. Available at:
Zwick, D., 2015. Simulation and Optimization in Offshore Wind Turbine Structural Analysis. NTNU-Trondheim Norwegian University of Science and Technology.